arXiv:cond-mat/0208119v1 [cond-mat.str-el] 6 Aug 2002

Spin order on pyrochlore lattices studied by the Self-Consistent Cluster Approach.

Wiebe Geertsma,
UFES-CCE/Depto de Fisica,
Fernando Ferrari s/n, Campus Goiabeiras,
29060–900 VITORIA–ES (Brasil);

November 7, 2021

Abstract

In this paper we present a study of magnetic order of quantum Heisenberg spins on *pyrochlore* type lattices: a lattice of corner sharing tetrahedra. We use the Cluster Variation Approximation with the tetrahedron as basic cluster. We find that in case of anti-ferromagnetic nearest–neighbour exchange there is no long–range spin order at any finite temperature for any spin **s**. For ferromagnetic exchange and $s = 1/2$ the spin system remains in a non-magnetic phase for all temperatures, while for $s > 1/2$ there is a finite order temperature. We derive the ground state phase diagram as a function of exchange anisotropy and tetragonal anisotropy and find regions of re–entrant behaviour. Magnetic fields can induce one or more magnetic transitions. Schottky–like anomalies appear in the specific heat, with on top signs of re–entrant behaviour. The limits of this Cluster Variation Approximations are discussed.

PACS: 75.10, 75.30E, 75.30H.
(Submit to Phys. Rev. B)
Keywords:theory, spin order, magnetism, insulators, .
Short title: Spin order on Pyrochlore lattices.

1 INTRODUCTION.

In this paper we report results for the critical temperature, susceptibility, magnetization and specific heat for Quantum Heisenberg spins ($s = 1/2$ to $s = 7/2$) on the highly frustrated pyrochlore lattice using the Cluster Variation Approximation (CVA). This pyrochlore lattice is a lattice with Corner Sharing Tetrahedra (CST) which has the highest known degree of frustration according to Lacorre's definition [1].

In the last decade the properties of spins on this pyrochlore lattice (see figure 1) have received much attention because it promises to be a realization of a 3D Quantum Spin Liquid (QSL) with possibly exotic ground states. Investigated Quantum ground states are for example based on singlet valence bonds, leading to a Resonating Valence Bond (RVB) system, introduced by Anderson [2, 3] for a 2D triangular lattice, or a Valence Bond Solid/Crystal, or order based on a singlet tetrahedron (=RVT) or plaquette state, or the formation of a ground state with long range chiral order.

One of the basic features of such frustrated spin lattices is their extensive residual or zero–point entropy at $T = 0$, or formulated in another way - a macroscopic degenerate ground state, with a degeneracy $\propto a^N$, where $a > 0$ and N is of the order of Avogadro's number. The consequences of this degeneracy are many: 1) a large decrease of the ordering temperature T_c, such that $f = \Theta_{CW}/T_c \gg 1$, where Θ_{CW} is the asymptotic Curie–Weiss temperature [4, 5]; in the region below the classical Mean–Field transition temperature the spins enter in a highly correlated quantum state, which in the case of classical spins is called a "cooperative paramagnet" [6], and a possible spin freezing below T_F into a Spin Glass phase [7, 8, 9]; 2) a shift of spectral weight to low energies from high energies of the order of Θ_{CW} [10]; 3) Schottky–type anomalies in the specific heat in case there are no states in the singlet–triplet gap and a specific heat $\propto T^n$ with singlet states in the singlet–triplet gap, while the susceptibility is always thermally activated ; 4) small external perturbations can lift (part) of the ground state degeneracy and thereby may radically change the type of (exotic) ground state: for example lattice distortions related to a Jahn–Teller effect [11, 12] bond disorder [13], field induced order [14, 15, 16] or the formation of a spin glass phase; 5) order-by-disorder: such small perturbations can also be quantum and/or thermal fluctuations (entropic ground states selection) [17, 18, 19]; 6) anomalous, non-universal, critical properties [20]; 7) peculiar spin dynamics [21]; 8) in case of Ising spins quantized along the local $< 111 >$ axis a cubic spin–ice type ground state [22, 23], which, in case that the dipole–dipole interactions are stronger than the exchange interactions, is described as Dipolar–Spin–Ice [24, 25, 26, 27]

Reviews of experimental work on the susceptibility of Rare–Earth Stannate pyrochlores can be found in [28], for the magnetic properties of compounds with a pyrochlore spin lattice in [29], and for the bulk magnetization of Rare–Earth Titanate pyrochlores in [30, 4]. Reviews of theoretical work are given by Bramwell and Gingras [31], Moessner [6], and a review by Lhuillier and Misguich [32] where the pyrochlore system is discussed in the perspective of the general class of frustrated quantum spin systems.

Anderson [33] started the study of order on the pyrochlore lattice and compared it with the positional disorder of H in hexagonal ice. He predicted the absence of Ising-type order down to $T = 0$ in case of antiferromagnetic nearest–neighbour interactions for spins quantized along a tetragonal axis, calling such a system "Cubic–Ice" [34, 35]. We

can sum up the present understanding of the Classical Antiferromagnetic Heisenberg spin $s = 1/2$ on the pyrochlore lattice as follows: this spin system does not order from the point of view of classical spins: the highest $J(\mathbf{q})$ modes are two–fold degenerate without any dispersion [36, 37, 38], meaning that below the mean-field ordering temperature $T_{c,MF} = 4/3J_{nn}$ the spin system moves in these modes, thereby using only 1/2 of the total number of degrees of freedom. Moessner and Chalker [39, 40] showed by an explicit construction procedure that all ground state configurations are connected, without any energy barrier. However certain correlations remain, which give rise to certain features in the neutron scattering: a few long-range correlations in high–symmetry directions is build into the ground state.

Various authors have studied possible "order–by–disorder" in this lattice, introducing thermal or quantum fluctuations on top of the classical ground state, see for example [19]. Most authors, probably starting with Reimers [37], first diagonalize the Heisenberg antiferromagnetic spin Hamiltonian with nearest–neighbour exchange on an isolated tetrahedron and then construct the pyrochlore lattice with these non-overlapping tetrahedra, and introduce the interaction between these tetrahedra as a perturbation: λJ_{nn}. The tetrahedron–tetrahedron interaction has been calculated up to 3rd order in λ. Garcia–Adeva and Huber [41] used the most simple approach by neglecting these tetrahedron–tetrahedron interactions: in this way long–range order is excluded from the outset. The asymptotic "Curie–Weiss" temperature found is 1/2 of the value obtained from the canonical mean field approximation. Canals and Lacroix [42, 43] performed a density matrix expansion up to λ^3 and found that at this order the degeneracy is weakly lifted ($\propto 10^{-6}J$) giving rise to a collinear AF spin structure: the spins along $< 110 >$ are parallel while nearest–neighbour perpendicular $< 110 >$ crossings are antiparallel. The correlation length is at most of the order of one lattice spacing. Their approach can not elucidate the character of the ground state: whether it has long range order in one of the exotic ground states mentioned above.

Several authors have discussed this possibility by calculating the tetrahedron–tetrahedron interactions in the restricted space of the two–fold degenerate singlet states and 3–fold degenerate triplet states of the tetrahedron. The latter are essential for inter–tetrahedron interactions. Although starting from different points of view, the ground state of this spin system seems to be some singlet–dimer covering of the pyrochlore lattice: Tsunetsugu [44] used a chiral ansatz and found vanishing chirality: the ground state is a four sublattice system of tetrahedra with singlet dimer order on three sublattices each occupied by one of the possible tetrahedron singlet dimer states, and the 4th sublattice is locally disordered.The ground state of the singlet dimer lattice can be characterized as a Valence Bond Solid. Singlet excitations will appear in the singlet–triplet gap: these are oscillations in the dimer pattern. A similar ground state has been found by Eljahal *et al* [45], by Isoda and Mori [46]. A dimer covering was already discussed by Harris *et al* [47]. Recently Berg *et al* [48] pushed this approach one step further and used the two–fold degenerate singlet ground state of a super tetrahedron - consisting of 4 tetrahedra connected each by different bonds - as a basis for a perturbation calculation. To each super tetrahedron is assigned a pseudo spin, these super tetrahedra form a bcc lattice. From a Monte–Carlo study, treating these pseudo spins as classical entities. They find that the ground state is ordered anti ferromagnetically, with ferromagnetic layers.

Adeva-Garcia and Huber[49] have studied the magnetic properties of spins on the pyrochlore lattice using the constant–coupling approximation and recently applied it to $ZnCr_2O_4$[8]. The same authors studied the critical properties of these pyrochlore spin systems using a Renormalization Group appraoch[50].

When one looks into the pyrochlore structure one finds that each atom on this lattice shares six planar hexagons, two in each $<111>$ direction, of which each of the three pairs of hexagons are edge sharing. The hexagons in a (111) plane form a Kagomé lattice. So this pyrochlore lattice also may be characterized as a lattice of inter-penetrating Kagomé lattices.

Let us now turn our attention to *nn* ferromagnetic interactions. There is at first sight no reason why the spins on a lattice of CST would not order at finite temperature. First consider the case that the spins are Ising spins pointing along the local $<111>$. In that case there are six degenerate states with a two-spin-in two-spin-out configuration on each tetrahedron [22, 23] and the spin states can be mapped on a model describing the two possible positions of Hydrogen in the ice structure [34]. This leads to so–called ice rules for the possible low temperature spin configurations. A clear exposition of these rules and its consequences can be found in [22, 23, 51]. Because of this ground state degeneracy, the entropy at $T = 0$ K is finite, and the macroscopic ground state of this spin system is called spin–ice.

In the present paper we apply the Cluster Variation Approximation (CVA) for the configurational entropy, in which one divides the lattice in a set of overlapping clusters[52, 53] (basis cluster) to study the magnetic properties of Quantum Heisenberg spins on a pyrochlore lattice. We use the tetrahedron as basis cluster. We include tetrahedral anisotropy, and an anisotropy in the exchange interactions caused by a tetragonal distortion of the lattice. Single–ion anisotropy and dipole–dipole interactions are discussed briefly.

Recently this approach has been applied to the problem of classical Ising spins on a pyrochlore lattice by Yoshida et al [54]. The properties of this classical Ising model are quite different from the ones we report in this paper, especially the ground state degeneracy.

The CVA is simply the Mean Field approximation in case the basic cluster is a single site. In case the whole crystal is taken as the basic cluster the approximation becomes exact. In between one has to make an intelligent choice for the basic cluster: we have chosen the tetrahedron as the basic cluster. The tetrahedron is the smallest unit possessing all the symmetry of the lattice, it is the unit which seems to contain the basic magnetic properties of the spin system: the high frustration against order in case of AF order. Another appealing property is that one can easily diagonalize the spin Hamiltonian for such a cluster, and the Clebsch–Gordan coefficients are also easily calculated.

The hexagons next to the triangles, are the smallest self-avoiding closed loops on the pyrochlore lattice. So any description based only on the tetrahedral clusters, means we neglect these hexagon closed loops. In this sense our approximation is similar to that for a Husimi tree [55] lattice, although our approximation does not suffer from the rather peculiar increase in the number of surface clusters, see also [56].

This paper is organized as follows. In section 2 we introduce and discuss qualitatively a Hamiltonian describing the spins on this pyrochlore lattice. We transform the site

Hamiltonian to a Hamiltonian for tetrahedra (2.1). In section 2.2 we discuss the spectrum of a 16 site cluster. We then derive in section 2.3 the susceptibility for a pyrochlore lattice covered with non interacting tetrahedrons. In section 2.4 we give some basic details of how we apply the CVA to this Heisenberg Quantum system. We derive an expression for the (linear) susceptibility (2.4.2). In the next section 3 we present first the critical temperature (3.1) and we present the zero temperature phase diagram for ferromagnetic and AF *nn* interactions (3.2), and then present the principal numerical results on the susceptibility, magnetization as a functioon of magnetic field and temperature (3.3). In a final section 4 we give a brief summary and conclusions.

2 THEORY.

The general Hamiltonian to describe spin–spin interactions is the Heisenberg Hamiltonian. We consider nearest–neighbour (J_{nn}), and briefly we will also discuss qualitatively the consequences of next–nearest–neighbour (J_{nnn}), and next–next–nearest–neighbour (J_{nnnn}) exchange interactions. We assume that each of these interactions does not depend on the details of the interaction path in the pyrochlore structure: *nn*, *nnn*, and *nnnn* indicates by how many cation–cation links these cations are separated. From an analysis of ESR spectra of Cr^{3+}–doped spinel $ZnGa_20_4$ Henning [57] derives the Cr^{3+}–Cr^{3+} exchange constants on this spinel B sublattice. These exchange constants show only small deviations – of about 10 % – from the average value of each type of exchange path. We also consider the possibility of local single–ion trigonal and tetragonal anisotropy. In case of the single–ion anisotropy the local trigonal field is along a local $<111>$ axis pointing to the center of the tetrahedron. The tetragonal anisotropy can be due to a tetragonal distortion, due to uni-axial pressure, of the cubic pyrochlore or spinel structures. It will be accompanied by a change in the two *nn* exchange interaction in the {100} planes with respect to the other four *nn* exchange interactions in the {111} planes (see figure 2). The Hamiltonian for this spin system in a magnetic field $\mathbf{H}$ reads:

$$\begin{aligned} H &= J_{nn}\sum_{i,j}\mathbf{s}_i\cdot\mathbf{s}_j + J_{nnn}\sum_{i,j}\mathbf{s}_i\cdot\mathbf{s}_j + J_{nnnn}\sum_{i,j}\mathbf{s}_i\cdot\mathbf{s}_j + \Delta\sum_{i,j;pairs}\mathbf{s}_i\cdot\mathbf{s}_j \\ &\quad + D_{0s}\sum_i(\mathbf{s}_i'^{\,2} - 3s_{iz}'^{\,2}) + D_T\sum_\alpha(\mathbf{S}_\alpha^2 - 3S_{\alpha\,z}^2) + \sum_i g\mu_B\mathbf{H}\cdot\mathbf{s}_i, \end{aligned} \tag{2.1}$$

The fourth contribution is a sum over the exchange interactions in the {100} planes. We reserve capitals $\mathbf{S}_\alpha$ for the size of the cluster (tetrahedron) spins and small $\mathbf{s}$ for the local atomic spins. The magnetic field $\mathbf{H}$ in the last term is along a tetragonal axis (see figure 2).

The $\mathbf{s}'$ in the single–ion contribution D_{0s} term indicates quantization of the spin along the local trigonal $<111>$ axis. In case the single–ion anisotropy $D_{0s} > 0$ the local $<111>$ axis is the easy axis, while in case $D_{0s} < 0$, the spin rotates in the $x'y'$ plane perpendicular to this axis. In case $D_{0s} > 0$ and much larger than the exchange interactions it is often argued that one may approximate the spins as classical (Ising) spins [58]. In case of a tetragonal distortion along one of the S_4 axes of the tetrahedron one finds

$$H_{si} = \frac{1}{2}D_{0s}(3\cos^2\theta_4 - 1)\sum_i(\mathbf{s}_i^2 - 3s_{iz}^2) \tag{2.2}$$

$$-3\sqrt{2}D_{0s}\cos\theta_4\sin\theta_4\left[s_{1z}s_{1+}+s_{1+}s_{1z}-s_{2z}s_{2+}-s_{2+}s_{2z}+i(s_{3z}s_{3-}+s_{3-}s_{3z}-s_{4z}s_{4-}-s_{4-}s_{4z})\right]$$
$$-\frac{3}{2}D_{0s}\sin^2\theta_4\left[(s_{1+}^2-s_{1-}^2)+(s_{2+}^2-s_{2-}^2)-(s_{3+}^2-s_{3-}^2)-(s_{4+}^2-s_{4-}^2)\right]$$

where θ_4 is indicated in figure 2. The single–ion anisotropy vanishes in case $s = 1/2$.

Next let us briefly discuss the tetragonal anisotropy D_T. When the tetrahedral anisotropy $D_T > 0$, the tetrahedron spin S is aligned along a tetrahedral axis, and in case $D_T < 0$, this spin is rotating in the plane perpendicular to a tetrahedral axis. This term can also be written in terms of the single–site spins:

$$\begin{aligned}&(J_{nn}+D_T)\sum_{<i,j>}s_is_j-3D_T\sum_{<i,j>}s_{iz}s_{jz}+2D_T\sum_i(s_i^2-3s_{iz}^2)=\\&(J_{nn}-2D_T)\sum_{<i,j>}s_{iz}s_{jz}+(J_{nn}+D_T)\sum_{<i,j>}(s_{ix}s_{jx}+s_{iy}s_{jy})+2D_T\sum_i(s_i^2-3s_{iz}^2).\end{aligned}\tag{2.3}$$

The tetrahedral anisotropy interpolates between a Ising model ($J_{nn} = -D_T$) and an XXZ model to a Heisenberg ($D_T = 0$) and XX model ($J_{nn} = 2D_T$), by changing the ratio D_T/J_{nn}. In the next section we will get more insight in this term by writing the whole Hamiltonian in terms of tetrahedron spins.

2.1 The Tetrahedron Approach.

2.1.1 The Hamiltonian.

For the CVA with the tetrahedron as a basic cluster we need the spin states of this tetrahedron. We define for tetrahedron α the total spin as $\mathbf{S}_\alpha = \mathbf{s}_1 + \mathbf{s}_2 + \mathbf{s}_3 + \mathbf{s}_4$. For the Δ term we introduce $\mathbf{L} = \mathbf{s}_1 + \mathbf{s}_2$ and $\mathbf{R} = \mathbf{s}_3 + \mathbf{s}_4$. One can now rewrite the exchange part and magnetic field of the original Hamiltonian in terms of these tetrahedron spins

$$\begin{aligned}H &= (J_{nn}-2J_{nnn}+3J_{nnnn})\sum_\alpha\mathbf{S}_\alpha^2+(J_{nnn}-2J_{nnnn})\sum_{(\alpha,\beta)_{nn}}\mathbf{S}_\alpha\cdot\mathbf{S}_\beta+J_{nnnn}\sum_{(\alpha,\beta)_{nnn}}\mathbf{S}_\alpha\cdot\mathbf{S}_\beta\\&+\frac{1}{2}\sum_\alpha g\mu_B\mathbf{H}.\mathbf{S}_\alpha+\Delta\sum_\alpha\left(\mathbf{L}_\alpha^2+\mathbf{R}_\alpha^2\right)+D_T\sum_\alpha(\mathbf{S}_\alpha^2-3S_{\alpha z}^2)+H_{si}\end{aligned}\tag{2.4}$$

The sum is over all tetrahedra in the lattice, including the ones which share a corner: so in case of the pyrochlore lattice there are $N/2$ CST. The sum over α and β is over all tetrahedra under the condition that they are *nn* or *nnn* tetrahedra. We have dropped terms of type $J\sum_i s_i^2$, as these only add a constant energy to the Hamiltonian. The first term gives the energy levels of an isolated tetrahedron, with an effective exchange in one tetrahedron of $J_{nn} - 2J_{nnn} + 3J_{nnnn}$. This correction on J_{nn} should only be taken into account when also the the corresponding *nn* and *nnn* are taken into account: the second and third terms give these interactions between the total spins on *nn* and *nnn* tetrahedra.

We note that several of these contributions (D_T, Δ) also appear in a summation of the dipole interaction within a tetrahedron:

$$H_D=\frac{D_D}{8}\left[\mathbf{S}^2-3S_z^2\right]+\frac{2D_D}{3}\left[L^2+R^2-3(L_z^2+R_z^2)\right]+\cdots\tag{2.5}$$

where $D_D = g^2\mu_B^2/R^3$, R is the interatomic distance in a tetrahedron. The dipole interaction, diagonal in the tetrahedron cluster states, is taken into account (except a contribution of the form $L_z^2 + R_z^2$), the last term in eq. 2.5. All single and double spin flip terms appearing in the dipole–dipole interaction are not taken into account. These contributions cause the dipole–dipole interaction neither to commute with M_s, nor with S^2.

2.2 The eigenstates of five coupled tetrahedra.

In order to discuss the ground state of a lattice of CST, we calculated the ground state of a finite cluster consisting of 4 outer tetrahedra each sharing a corner with the same central tetrahedron: 5T super-tetrahedron. First let us briefly consider the energy levels of the tetrahedron. These are in figure 3 and table 1. In case of nn AF xchange interactions the ground state is a degenerate pair of singlets and in case of F interactions a quintet state $S = 2$. This pair of singlet states is split by the $L^2 + R^2$ perturbation into two singelts, one with $L = 0$, $R = 0$: the two dimer singlet state, and the other $L = 1$, $R = 1$: the plaquette or tetrahedron Singlet state. Also the dipole–dipole interaction splits this singlet.

We calculate the ground state energy in case of AF interactions. We proceed as follows: the Heisenberg Hamiltonian is rewritten in terms of the tetrahedron spins S_i, for the outer 4 tetrahedra. The eigenstates can easily be found using the Clebsch-Gordan coupling coefficients. These states are represented by the following set of quantum numbers: $|Q, M_Q, D_1, D_2, S_1, S_2, S_3, S_4, L_1, R_1, L_2, R_2, L_3, R_3, L_4, R_4\rangle$, where Q and M_Q are the total spin and magnetic moment of the outer 4 tetrahedra, D_1 is the spin of the tetrahedra with S_1 and S_2, and D_2 of S_3 and S_4. The L_i and R_i are defined above. This basis is diagonal in the Hamiltonian for the exchange interactions of the outer four tetrahedra. The 6 exchange interactions in the central tetrahedron have now to be considered separately. For $M_Q = 0$, and $Q = 8$, 7, 6, 5, this can be done easily. For the other M_Q values we have chosen the following scheme in order to determine the ground state and first excited states: we choose a maximum value for S_i, D_i and Q, for $M_Q = 0$ and restrict the sum over all tetrahedron spins S_i. That is, we restrict the number of singlet–triplet–quintet excitations in the cluster. Our results for the ground state energy E_{GS} and singlet–triplet gap Δ_{ST} are in table 2. We find that the ground state is a set of 16 singlets. There is only coupling between the four outer tetrahedra by singlet–triplet excitations. We find $E_{GS} = -12.82J$ for our T5 super-tetrahedron, which is $-0.81J$/site. This value is smaller then obtained for the 16 site super-tetrahedron of Berg *etal* [48]. The singlet–triplet gap is about $\Delta_{ST} = 1.56J$, which means a decrease of about 25 % with respect to independent tetrahedra. In table 3 we have collected some data from recent calculations of these quantities.

The ground state degeneracy of the T5 cluster is determined by the 2–fold degenerate ground-state of singlets of each of the 4 outer tetrahedra. The state on the central tetrahedron is completely determined by the state on each of the four outer tetrahedra. When we extend this description to the complete pyrochlore lattice – which is from the point of view of the tetrahedra a diamond lattice – the ground state is $2^{N/4}$–fold degenerate for a lattice of N sites in case of AF interactions.

In our calculations on the T5 cluster we observed a partial lifting of the degeneracy

for certain choices of the restriction on the maximum number of excitations (the size of Hilbert space): to get the correct degeneracy one has to diagonalize the complete matrix. In this T5 cluster we do not find lifting of the degeneracy due to inter-tetrahedron interactions [21]. Diagonalization of only part of Hilbert space gives incorrect degeneracies and spurious eigenvalues.

Such singlet gap-states seem to appear as a function of the cluster size, or in a real system as a function of the spin–spin correlation length. This implies that the extent of spin singlet states depends on temperature, and the singlet–singlet excitation spectrum collapses to a single highly degenerate level or a narrow band ($\ll J$) of singlet states: that is, transfer of spectral weight from high to low frequencies with decreasing temperature. The appropriate correlation lenght if this quantum order increases with decreasing temperature. At high temperature ($T \geq J$) this correlation lenght is of the order of one interatomic distance.

2.3 The paramagnetic susceptibility of independent tetrahedra.

With *nn* exchange interactions J only, and neglecting the restrictions due to corner sharing of spins, one derives easily the following expression for the susceptibility[41]:

$$\chi = \frac{g^2\mu_B^2}{k_BT} J \frac{\sum_S g_S S(S+1)(2S+1)\exp(-E_S/k_BT)}{\sum_S g_S(2S+1)\exp(-E_S/k_BT}, \tag{2.6}$$

where g_S is the degeneracy of a tetrahedral S-state excluding the $(2S+1)$ degeneracy which is included explicitly in this expression. The energy of each S state is given by

$$E_S = JS(S+1). \tag{2.7}$$

In the high temperature limit one derives:

$$\chi_{HT} = \frac{g^2\mu_B^2}{3k_BT} \frac{G_1}{1-(G_1-G_2)J/k_BT}, \tag{2.8}$$

where

$$\begin{aligned} G_1 &= \frac{\sum_S g_S(2S+1)(S+1)S}{\sum_S g_S(2S+1)}, \\ G_2 &= \frac{\sum_S g_S(2S+1)(S+1)^2S^2}{\sum_S g_S(2S+1)(S+1)S}. \end{aligned} \tag{2.9}$$

One can now easily calculate the asymptotic Curie temperature:

$$\frac{k_B\theta_{CW}}{J} = \frac{1}{G_1-G_2}. \tag{2.10}$$

This asymptotic Curie temperature is not related to any long range order. For the case of $s = 3/2$ – for example Cr^{3+} with d^3 – one finds an asymptotic Curie temperature given by:

$$k_B\theta_{CW} = -\frac{15}{2}J, \tag{2.11}$$

which is 1/2 the value one would obtain from the usual Mean Field approximation! One finds the same factor 1/2 for the Kagomé lattice in case one treats the lattice as consisting of independent corner–sharing triangles.

2.4 The Cluster Variation Approximation with tetrahedron as basis cluster.

In this section we give some details of our calculation of the probability functions for quantum spins for the case of a tetrahedron cluster with $s = 1/2$. The calculation for higher spin values is only slightly different. The CVA is often applied to the classical problems of order–disorder transitions in alloys, and the problem of Ising spins. In the present case we apply it to the problem of Quantum Heisenberg spins. The approximation we make is that there is no coherence between the quantum states on different tetrahedra. At high temperature this leads to the classical Mean Field limit. However we will see that in certain cases below a certain temperature T_S the CVA breaks down: the entropy in this approximation becomes negative for $T < T_S$.

The states on the tetrahedron are written as linear combinations of the determinants: $|m_1 m_2 m_3 m_4|$, where m_i is the spin moment on i. The spin eigenfunctions can be written as:

$$|\Psi(S, M, L, R)\rangle = |\Psi(S, M, \alpha)\rangle = \sum_{m_1,m_2,m_3,m_4} \langle m_1, m_2, m_3, m_4|S, M, \alpha\rangle |m_1, m_2, m_3, m_4\rangle, \tag{2.12}$$

where $\langle m_1, m_2, m_3, m_4|S, M, \alpha\rangle$ are the Clebsch–Gordan coefficients. The α's indicate one of the eigenfunctions of the possible degenerate set of eigenstates with spin S and momentum M with different pairs (L, R). The restrictions are $|L - R| \leq S \leq L + R$, $M = M_R + M_L$, $0 \leq L \leq s_1 + s_2$, $0 \leq R \leq s_3 + s_4$, $M_L = m_1 + m_2$, $M_R = m_3 + m_4$.

The probability that a certain site has magnetic spin momentum m is:

$$x_m = \sum_{S,M,\alpha} a_{m;S,M,\alpha} y_{S,M,\alpha}, \tag{2.13}$$

where $y_{S,M,\alpha}$ is the probability that the tetrahedron is in one its eigenstates $|S, M, \alpha\rangle$, and $a_{m;S,M,\alpha}$ is the sum of the square of the (Clebsch–Gordan) coefficients of the states $|m_1, m_2, m_3, m_4\rangle$, with $m_1 = m$ in the expansion of the spin eigenstates of the cluster in terms of these determinants 2.12. For degenerate states it is important to symmetrize these coefficients, giving equal weight to each of these states.

The total average magnetic moment per site is now:

$$\langle m\rangle = g\mu_B \sum_m m x_m. \tag{2.14}$$

We define:

$$b_{m;S,M,\alpha} = a_{m;S,M,\alpha} - a_{m;0,0,\alpha_0}, \tag{2.15}$$

where the index α_0 is $(L, R) = (0, 0)$. These b-coefficients are in table 4. We define:

$$B_{m;S,M,\alpha} = a_{m;S,M,\alpha} - a_{-m;S,M,\alpha}. \tag{2.16}$$

The free energy of a system of N_t clusters on a lattice can be written:

$$F = N_t \sum_{\gamma} [\omega_\gamma E_\gamma - k_B T \ln W(\gamma)], \tag{2.17}$$

where E_γ is the energy of a cluster in state $\gamma = (S, M, \alpha)$, and $W(\gamma)$ is the number of ways to distribute a set of states $\{\gamma\}$, each occurring with probability ω_γ over the lattice.

In case of the tetrahedron as basis cluster, the number of ways to distribute these tetrahedron states over the lattice of CST is calculated as follows: first distribute these tetrahedron states over the whole lattice. Z_t tetrahedra will share the same corner. So there are $N_t = Z_t/4N$ tetrahedra, each characterized by a spin eigenstate on the lattice. The number of ways of putting these tetrahedron spin states on the lattice is:

$$Q = \frac{N_t!}{\prod_\gamma (N_t y_\gamma)!} \tag{2.18}$$

In order that a certain distribution belongs to a realizable one, the local spin moment for each of these tetrahedra should be the same on the shared atoms, called the overlap cluster. In case of the pyrochlore lattice the overlap cluster is the point cluster, and $Z_t = 2$.

This restriction on the distribution of these tetrahedron spin states can not be applied rigorously, but on the average: the CVA for the entropy. At high temperatures the spins are distributed over all spin eigenstates of the tetrahedron: this is the classical regime of spin fluctuations. At very low temperature, when the tetrahedron spins are distributed over a small number of tetrahedron spin states, one is in the regime of quantum spin fluctuations. In case no classical long–range spin order interferes this classical approximation of the entropy can break down. In case the degeneracy of the tetrahedron ground-state is too low, the entropy within the CVA is negative below a certain temperature. When, at low temperature, the tetrahedron ground-state is a single non degenerate singlet state, no correction is necessary: due to quantum spin fluctuations the average spin on each site vanishes: there is self–averaging. The description of such a state is outside the validity regime of the CVA. We take into account correlated spin fluctuations of the size of the tetrahedron, correlated spin fluctuations over larger distance are not described within the present approach. With this self–averaging one might argue that in a certain temperature range before the system enters the regime of correlated spin fluctuations, the state on *nnn* tetrahedra are independent and one could approach the susceptibility by eq. 2.6. If that is the case the asymptotic Curie–Weiss temperature found from magnetic susceptibility data at relative low temperature gives an exchange interaction 1/2 the actual value.

The correction within the CVA is now calculated as follows. Distributing N_t tetrahedra over the pyrochlore lattice generates $Z_t N$ spins. On each site of the pyrochlore lattice there are $Z_t = 2$ spins, which we call pseudo sites. First calculate the number of ways of putting $Z_t N$ spins with at any moment either spin up or down on the lattice of $Z_t N$ pseudo sites. Of these arrangements, only a fraction is correct: all spin momenta on the Z_t pseudo sites belonging to the same site are the same. Now the average fraction of correct point configurations is:

$$\Gamma = \left[\frac{(N)!}{(x_{-1/2}N)!(x_{1/2}N)!} \right]^{1-Z_t}. \tag{2.19}$$

Combining this correction with the number of arrangements of the tetrahedron configurations on the pyrochlore lattice we obtain for the average number of correct arrangements

$$W = (N!)^{1-3Z_t/4} \left[\frac{1}{\prod_\gamma (Ny_\gamma)!}\right]^{Z_t/4} \left[\frac{1}{(x_{-1/2}N)!(x_{1/2}N)!}\right]^{1-Z_t}. \tag{2.20}$$

In case of $s > 1/2$ one should replace the product $(x_{-1/2}N)!(x_{1/2}N)!$ by the appropriate product for spin s: $\prod_{m=-s,s}(x_m N)!$.

Substitution of this equation for the total number of spin configurations in the expression for the free energy and using Stirling's formula for large N we obtain for the free energy per site

$$\begin{aligned} f = F/N &= Z_t/4 \sum_\gamma y_\gamma E_\gamma \\ &+ k_B T \left[Z_t/4 \sum_\gamma y_\gamma \ln(y_\gamma) + (1-Z_t) \sum_{m=-s,s} x_m \ln(x_m) \right]. \end{aligned} \tag{2.21}$$

In order to obtain the equilibrium values for the probability functions we have to minimize the free energy with respect to these functions y_γ, and find:

$$0 = \frac{\partial f}{\partial y_\gamma} = Z_t/4 \left[(E_\gamma - E_0) + k_B T \left(\ln \frac{y_\gamma}{y_0} + \frac{4(1-Z_t)}{Z_t} \sum_{m=-s,s} \frac{\partial x_m}{\partial y_\gamma} \ln(x_m) \right) \right], \tag{2.22}$$

where we used the fact that these distribution functions x and y are normalized. y_0 and E_0 indicates the state with $S = 0, L = 0, R = 0$. Using the definitions of the coefficients we can write: $\frac{\partial x_m}{\partial y_\gamma} = b_{m;\gamma}$. We eliminate the state 0 from these equations and write for the energy of the eigenstates in a magnetic field:

$$E_{S,M,\alpha} = E^0_{S,M,\alpha} + g\mu_B M H. \tag{2.23}$$

where $E^0_{S,M,\alpha} = E^0_{S,-M,\alpha}$. The equilibrium equations become:

$$\frac{y_{S,M,\alpha}}{y_{S,-M,\alpha}} = \prod_m x_m^{2C_t\, B_{m;S,M,\alpha}} \exp(2Mh/T), \tag{2.24}$$

where we defined: $h = g\mu_B H$, and we set $k_B = 1$ and the constant $C_t = 2(Z_t - 1)/Z_t$.

In case the spin system is non–magnetic – no long–range order – one can easily solve these equations. The distribution functions are independent of the magnetic quantum number M, and the probability that a spin is in one of its $2s+1$ magnetic moment states m is in case of Heisenberg spins: $1/(2s+1)$.

In case of finite single–ion anisotropy, the x_m should be evaluated using the appropriate probability distributions for the non–magnetic solution.

The distribution over the tetrahedron states is in the non–magnetic case without magnetic field given by:

$$y_{S,M,\alpha} = y_0 \exp(-(E_{S,M,\alpha} - E_0)/k_B T), \tag{2.25}$$

and

$$y_0 = 1 - \sum_{S,M\alpha \neq 0} y_{S,M,\alpha}. \tag{2.26}$$

2.4.1 The entropy $\mathcal{S}$ for $s = 1/2$.

The free energy is for $s = 1/2$ in the disorder regime:

$$F = -\frac{1}{2} k_B T \ln Z_0 + k_B T \ln 2 \tag{2.27}$$

and the entropy in this regime is:

$$\mathcal{S}/k_B = \frac{1}{2} \ln(Z_0/4) + \frac{1}{2} T \frac{d \ln Z_0}{d T} \tag{2.28}$$

where

$$Z_0 = \sum_{\gamma} \exp(-E_\gamma / k_B T) \tag{2.29}$$

In the disorder regime the single–site spin momentum probabilities $x_{m=\pm 1/2} = 1/2$ are constant. For $T \to 0$ the last contribution to the entropy can be neglected. We find that for $Z_0 < 4$ the entropy becomes negative: the restrictions imposed by the CVA are too strong. The temperature where this occurs we call T_S. We find that in case there is no long–range order at any finite temperature, then in case the tetrahedron has a ground state with a degeneracy less than 4, the spin system has in some way to enter a state of correlated spin motion in order to satisfy the thermodynamic requirement that $\mathcal{S} \geq 0$. Already far above T_S one should observe strongly correlated spin fluctuations extending over more than one tetrahedron.

It seems that the restrictions to determine the number of realizable configurations imposed by the CVA are too strong. At low temperatures, when only singlet tetrahedron states are occupied, there is self–averaging and no CVA–type restrictions are necessary.

2.4.2 The magnetic susceptibility.

In order to calculate the magnetic susceptibility we linearize the functions which describe the distribution of the spin configurations in the magnetic field H and the magnetization $\mathcal{M}$ as follows. First we write:

$$y_{S,\pm M,\alpha} = y_{0;S,M,\alpha}(1 \pm m_{S,M,\alpha}), \tag{2.30}$$

where $m_{S,M,\alpha}$ is a new function linear in the magnetization and magnetic field. In the following the summations over M are restricted to $M \geq 0$. We linearize the exponent which contains the magnetic field and get:

$$(1 + 2m_{S,M,\alpha}) = (1 + 2Mh) \prod_{m=-s,s} x_m^{-2C_t\, B_{m;S,M,\alpha}}. \tag{2.31}$$

Next we write an expression for the single–site distributions in terms of these cluster distributions, and we find

$$x_m = x_{0,s,m} + \sum_{S,M>0,\alpha\neq 0} B_{m;S,M,\alpha}\, y_{S,M,\alpha}\, m_{S,M,\alpha}, \tag{2.32}$$

where we defined

$$x_{0,s,m} = \sum_{S,M,\alpha\neq 0} b_{m;S,M,\alpha} y_{S,M,\alpha} + b_m(0). \tag{2.33}$$

We have now reduced the number of unknown state distribution functions to the states without taking into account the M degeneracy. For $s = 1/2$ there are 6.

One can easily see that $B_m = -B_{-m}$. So we can write ($h = H/k_BT$):

$$\begin{aligned} 1 + 2m_{S,M,\alpha_S} &= (1 + 2Mh) \\ &\left[\frac{\prod_{m>0}\left[x_{0s} + \sum_{S,M>0,\alpha\neq 0} B_{m;S,M,\alpha} y_{S,M,\alpha} m_{S,M,\alpha_S})\right]}{\prod_{m>0}\left[x_{0s} - \sum_{S,M>0,\alpha\neq 0} B_{m;S,M,\alpha} y_{S,M,\alpha} m_{S,M,\alpha})\right]}\right]^{-2C_t\ B_{m;S,M,\alpha}} \end{aligned} \tag{2.34}$$

This can now easily be evaluated to lowest order in the magnetic field and the magnetization for each m state. We define the following quantity:

$$m_m = \sum_{S,M>0,\alpha\neq 0} B_{m;S,M,\alpha} y_{S,M,\alpha} m_{S,M,\alpha}, \tag{2.35}$$

and we can now solve for m_m:

$$m_m = K_m h - C_t \frac{2}{x_{0s}} Y_m m_m - C_t \frac{2}{x_{0s}} \sum_{m_1\neq m; m_1>0} Y_{mm_1} m_{m_1}, \tag{2.36}$$

where we defined the following functions:

$$K_m = \sum_{S\neq 0,M>0,\alpha} B_{m;S,M,\alpha} M y_{S,M,\alpha}, \tag{2.37}$$

$$Y_{m_1 m_2} = \sum_{S\neq 0,M>0,\alpha} B_{m_1;S,M,\alpha} B_{m_2;S,M,\alpha} y_{S,M,\alpha}. \tag{2.38}$$

In the cases $s = 1/2$ and $s = 1$ this set of equations can be solved easily. In the case $s = 1/2$ one finds

$$m_{1/2} = K_{1/2}/(1 + C_t \frac{2}{x_{0,1/2}} Y_{1/2})h, \tag{2.39}$$

with $x_{0,1/2} = 1/2$.

The magnetization can be written as:

$$\mathcal{M} = \sum_m m x_m = 2 \sum_m m m_m \tag{2.40}$$

The second equation for $\mathcal{M}$ follows easily from the definition of x_m and m_m. The factor 2 appears, because the sum in m_m over M is only for $M > 0$.

The magnetic susceptibility is now given by:

$$\chi = \mathcal{M}/H = \frac{2\sum_m m m_m}{H} \tag{2.41}$$

and in case of spin $s = 1/2$ we get

$$\chi = \frac{m_{1/2}}{H} = \frac{K_{1/2}}{k_B T(1 + 4C_t Y_{1/2})} \tag{2.42}$$

The functions K and Y can easily be calculated from the Clebsch–Gordan coefficients and the probability distribution functions for the non–magnetic system. We find that the asymptotic Curie–Weiss temperature in the CVA is equal to the MF result.

For $s = 1/2$ we find for the susceptibility in case of zero uniaxial fields ($D_T = \Delta = 0$):

$$\chi = \frac{g^2\mu_B^2}{T}\frac{5e^{6J/T} + 3e^{2J/T}}{2 + 6e^{2J/T}}. \tag{2.43}$$

where we have set $k_B = 1$. A comparison of the CVA result and an exact high–temperature expansion shows that the CVA

$$\chi = \frac{g^2\mu_B^2}{T}\left[1 + 3x + 6x^2 + \frac{17}{2}x^3 \cdots\right] \tag{2.44}$$

already deviates at second order in $x = J/T$ [60]

$$\chi = \frac{g^2\mu_B^2}{T}\left[1 + 3x + 9x^2 + \cdots\right]. \tag{2.45}$$

We are not aware of any high–temperature expansion for the CST lattice, only for the Kagome [61].

The magnetization is given by the solution of the following implicit equation in $\mathcal{M}$:

$$\mathcal{M} = \frac{(A^-_{1,2} + \frac{1}{2}A^-_{\frac{1}{2},1})e^{\frac{6(J+D_T)+4\Delta}{T}} + A^-_{\frac{1}{2},1}e^{2\frac{J+D_T}{T}}\left(e^{2\frac{\Delta}{T}} + \frac{1}{2}e^{4\frac{\Delta}{T}}\right)}{1 + e^{4\frac{\Delta}{T}} + (A^+_{1,2} + A^+_{\frac{1}{2},1} + 1)e^{\frac{6(J+D)+4\Delta}{T}} + (A^+_{\frac{1}{2},1} + 1)e^{2\frac{J+D_T}{T}}\left(2e^{2\frac{\Delta}{T}} + e^{4\frac{\Delta}{T}}\right)} \tag{2.46}$$

where we defined: $x = (1 + \mathcal{M})/(1 - \mathcal{M})$, $A^{\pm}_{1,2} = (xe^{2H/T} \pm \frac{1}{x}e^{-2H/T})e^{-12D_T/T}$, and $A^{\pm}_{\frac{1}{2},2} = (\sqrt{x}e^{H/T} \pm \frac{1}{\sqrt{x}}e^{-H/T})e^{-3D_T/T}$.

3 RESULTS AND DISCUSSION.

3.1 The critical temperature for Heisenberg spins.

We determine the critical temperature as the temperature where the susceptibility diverges. The results are in table 5. In case $s = 1/2$ and only Heisenberg interactions, there is no magnetic long–range order at any finite temperature, neither for F nor for AF interactions. In our CVA to the pyrochlore lattice, AF Heisenberg spin interactions never give classical long–range order. In case of ferromagnetic Heisenberg interactions the CVA values are about 60 % of the usual Mean Field values, slightly increasing – as expected – for larger spin.

We calculated for $s = 3/2$ the critical temperature for F Heisenberg exchange from a high–temperature approximation [62] with 6 coefficients using the Padé extrapolation and find $T_c/J = -7.892$. Compared with this, in principle exact calculation, the CVA critical temperature is still too high, indicating that spin fluctuations are stronger than accounted for in our application of the CVA. Note also that our critical temperatures for ferromagnetic Heisenberg interactions are appreciably lower than those for the same coordination number using the interpolation equation of Rushebrook and Wood [63].

We studied the effect of increasing the number of tetrahedra sharing the same corner. We found that any increase however small will lead to a finite critical temperature for $s = 1/2$ in case of ferromagnetic Heisenberg exchange. This is illustrated in figure 5. A similar conclusion was reached by Pinettes et al [64] who – using MC simulations – analyzed the ordering temperature going from a pyrochlore to a fcc structure. They found that for very small values of the ratio of the extra exchange interaction – needed to transform the pyrochlore lattice into the fcc lattice – and the exchange interaction in the pure pyrochlore lattice, the system shows a collinear long–range order.

3.2 Ground state Phase Diagram for $s = 1/2$.

In order to derive the ground state phase diagram for $s = 1/2$ we calculated the energy levels of the spin states of the tetrahedron, which can be found in table 1 and are illustrated in figure 3. The phase diagrams in the d_T–δ plane, where $d_T = D_T/J$ and $\delta_T = \Delta_T/J$, are in figure 4 for ferromagnetic as well as antiferromagnetic interactions. We note that for various values of the distortion the ground state is non-magnetic. The lines separating the various regions can easily be found from the expressions for the energy.

In case of F interactions we find the following equations for the boundaries between the various ground states:
$(S = 0, M = 0)$–$(S = 2, M = 0)$: $2\delta + 3d_T + 3 = 0$;
$(S = 0, M = 0)$–$(S = 2, M = 2)$: $2\delta - 3d_T + 3 = 0$;
$(S = 2, M = 2)$–$(S = 2, M = 0)$: $d_T = 0$.
So we find 3 regions: one region where the spins show long–range order $(S = 2, M = 2)$, and two regions where we find a non magnetic ground state: one where the ground state of the spin system is build from singlet dimers ($S = 0$,$M = 0$,$L = 0$,$R = 0$), and one build from the nonmagnetic $M = 0$ component of the quintet state, indicated by RVT2.

In case of AF interactions we find the following boundary equations:
(S=2,M=2)–(S=0,M=0): $2\delta - 3d_T + 3 = 0$;
(S=0,M=0)–(S=2,M=0): $2\delta + 3d_T + 3 = 0$;
(S=0,M=0)–(S=2,M=0): $d_T = -1$;
(S=2,M=2)–(S=0,M=0): $d_T = 1$.

In this case we find four regions: the region with a classical long–range AF order, and three regions without magnetic long–range order, the region indicated by RVB in the diagram, with a ground state build up from singlet dimers, a region characterized by a singlet tetrahedron ground state with compensating triplet spins $L = 1$, $R = 1$, indicated by a Resonance Valence Tetrahedron state: RVT1, and a region where the ground state is build from the nonmagnetic spin moment $M = 0$ of the tetrahedron quintet state, indicated by RVT2.

In case of AF interactions and $d_T > 0$, the ground-state becomes magnetic for $d_T > d_{T,c} = (4s+1)/(8s+1)$. In case of $s = 1/2$ the critical value $d_{T,c} = 1$ and for very large s, $d_{T,c} \to 1/2$. If we translate this to the case that dipole–dipole interactions are the source of the tetragonal anisotropy, then $D_T = D_D/8$, and in the large s limit we find for the critical ratio of the nn exchange and the dipole–dipole interaction: $J/D_D = 1/4$. For smaller ratios the $S = 2, M = 2$ state drops below the singlet $S = 0, M = 0$ state. Whether

this can be applied to the Ising systems discussed in a recent review by Bramwell and Gingras [31], is not clear. In case we make the necessary corrections for J; their exchange interaction is -1.5 times our exchange constant, and we find from their work the following condition for magnetic order: $J/D < 1$, which is of the same order of magnitude as we have derived.

The boundary separating the magnetic from the non–magnetic solutions is not a sharp line: these two regions are separated by a re-entrant region where there are two critical temperatures. The extent of this region increases with increasing tetrahedron distortion like illustrated in figure 6. In figure 7 we give the critical temperature $k_B T_c/J$ as a function of the tetrahedral anisotropy d_T, for various values of the exchange anisotropy δ. This re-entrant behaviour is due to the occupation of a magnetic state with increasing temperature i.e. an entropic effect. It is a type order–by–disorder [17] transition: an increase in thermal spin fluctuations induces magnetic order.

Koga and Kawakami [65] have also derived a phase diagram for the Quantum Heisenberg pyrochlore system with AF interactions. They studied the influence of the exchange anisotropy Δ. When comparing their result with ours we might identify the plaquette state with our $S = 0, M = 0, L = 1, R = 1$ state and their dimer state with our $S = 0, M = 0, L = 0, R = 0$ state. For $\delta = 0$, for an undistorted tetrahedron these two states are degenerate. Whether the system with $\Delta = -J$ and AF interactions, i.e., the total L and R exchange interactions vanish, should show magnetic order is questionable. It is a very open 3D network with a very low coordination number of 4.

In figure 7 we compare the ferromagnetic order temperature T_c/J as a function of tetragonal anisotropy $d_T = D_T/J$ for various values of the exchange anisotropy $\delta = \Delta/J$. We find that $T_S < T_c$ in case of finite T_c.

In the regions of the phase diagram where the ground state has a degeneracy smaller than 4, there is a finite temperature T_S where the entropy in the CVA becomes negative. In figure 8 we present W -the number of states accessible by the spin system so that the entropy per site is $\mathcal{S}/k_B = \frac{1}{4} \ln W$ - for the case of ferromagnetic exchange $J = -1$ as a function of $T/|J|$, without any perturbations. Because the spin system does not order for $T > 0$, the entropy remains finite for all $T > 0$. At high temperatures the entropy approaches the value for a paramagnetic spin system ($\ln 2$).

We surmise that below T_S the spin system enters in a state with strongly correlated quantum spin fluctuations. The latter takes over from the slowed down thermal fluctuations. This occurs in all regions without magnetic moment degeneracy ($M = 0$).

Such a ground state degeneracy can also be lowered by a magnetic field. In figure 9 we present some results of T_S as a function of the tetragonal anisotropy for $\delta = 0$ and $\delta = -3$. In the first case the magnetic field favours the state with extended spin fluctuations for all d_T's while in case of $\delta = -3$ these fluctuations are suppressed with increasing field for small tetragonal anisotropy, while for large d_T the quantum correlated spin fluctuations are favoured by a magnetic field.

We have determined the extend of the re–entrant region for $s = 1/2$ to $7/2$. In fig. 10 we present the re–entrant region for $\delta =$ for $s = 3/2$. In table 6 we give T_{max}, $D_{T,max}$ values which characterize the extend of the re–entrant region for $s = 1$ to $s = 7/2$: this re–entrant region increases with increasing spin. We expect to find similar behaviour in case of trigonal single–ion anisotropy.

3.3 Magnetization $\mathcal{M}$ as a function of field and temperature: the F case.

In figure 11 we present the magnetization as a function of the magnetic field for ferromagnetic exchange ($J = -1$) and $s = 1/2$ along the lines A-C ($\delta = -3$ and B-D $\delta = 1$ in figure 4, for $T = 0.01|J|, 1|J|, 5|J|$. We can distinguish three types of behaviour, which is directly related to the ground state in the phase diagram.

1. In the region of (ferromagnetic) order ($S = 2$, $M = 2$) the magnetization behaves in the usual way as a function of the magnetic field. We note that for the unperturbed case ($\delta = 0$, $d_T = 0$) only a very small magnetic field is necessary to magnetize the system.

2. In the region characterized by ($S = 0$, $M = 0$, $L = 0$, $R = 0$), that is the region of the phase diagram where due to the δ and d_T anisotropy, the magnetic states are pushed far above the non magnetic ground state. Here we observe, at very low temperatures as a function of the magnetic field, a single first–order phase transition from a non–magnetic state to a completely ordered state: $\mathcal{M} = \mathcal{M}_{sat}$ for a field $h_c = -3 - 2\delta + 3d_T$. This transition smears out with increasing temperatures. At $T = 0$ this is what is called a Quantum Phase Transition.

3. The region characterized by ($S = 2$, $M = 0$, $L = 1$, $R = 1$). In this region the magnetization as a function of the field shows two first–order phase transitions as a function of the field at very low temperature: one at $h_{c1} = 3d_T$ and the next at $h_{c2} = 9d_T$ (Quantum Phase Transitions). The plateau in the magnetization is at $\mathcal{M} = 1/2\mathcal{M}_{sat}$. Like in the previous case these transitions are smeared out with increasing temperature.

Note that in various cases the magnetization increases nearly linear with the field, and in some case it changes from a convex to a concave function with increasing field.

These magnetic field dependences lead to a rather peculiar temperature dependence of the magnetization. In figure 11 we present the temperature dependence of the magnetization along the B-D line ($\delta = 1$) in the ferromagnetic phase diagram, for positive d_T values ($S = 2$, $M = 0$, $L = 1$, $R = 1$). Fundamentally we observe three types of behaviour of the magnetization as a function of the temperature. For small field the magnetization has a maximum as a function of the temperature for all values of $d_T > 0$. With increasing field for small values of d_T the system is ordered at low temperatures, while for large values of d_T the magnetization has a maximum. For intermediate values of d_T (see figure 11) the magnetization as a function of temperature exhibits a relative minimum. Note that in case this relative minimum is present in the magnetization as a function of temperature, than the zero temperature magnetization: $\mathcal{M}(T \to 0) \to 0.5\mathcal{M}_{sat}$, independent of the applied magnetic field. This is related with the plateau $\mathcal{M} = 1/2\mathcal{M}_{sat}$ in the magnetization as a function of field.

In the region ($S = 0$, $M = 0$, $L = 0$, $R = 0$) one only finds one peak in the magnetization as a function of temperature.

In figure 12 we present the magnetization in a small field for $\delta = -3$ for various values of the tetragonal anisotropy d_T in the re–entrant region. The peak in the magnetization

is clearly visible. Note that even outside the ordered region there is a finite magnetization which does not decrease to zero for vanishing field.

In figure 14 we illustrate the behaviour of the specific heat as a function of temerpature in the re–entrant region for ferromagnetic exchange. Note that there appear two peaks on top of a Schottky peak. The behaviour of the specific heat at low temperatures is uncertain as the CVA breaks down (negative entropy). We conjecture that trigonal perturbations can induce similar beaviour.

4 SUMMARY AND CONCLUSION

We conclude from our calculations that in case of AF *nn* exchange only there is no classical long–range spin order on the pyrochlore or B sublattice of the spinel structure at any finite temperature. This is a consequence of the high degree of frustration on this lattice for AF interactions and its low coodination number. In case of the simple cubic lattice, which has the same coordination number (6) as the pyrochlore lattice, there is spin order below a certain finite temperature with *nn* interactions only.

In case of F *nn* exchange only there is no spin order for finite temperatures for $s = 1/2$. For $s > 1/2$ one finds a finite critical temperature which is appreciably smaller than that found in the MF approach. However from a HTE using the coefficients in [66] one finds an even smaller ordering temperature, which indicates that even in the case of F *nn* Heisenberg–type interactions, spin order is frustrated. Such a frustration of spin order in case of F interactions has been discussed by Bramwell and Harris [22, 51] for the case of classical Ising spins, each pointing along the local $< 111 >$ axis of a tetrahedron: the 2 spin in 2 spin out ground state configuration is sixfold degenerate, leading to a finite zero temperature entropy. In case of quantum spins there is no such degeneracy. The reason why the $s = 1/2$ pyrochlore system with F interactions does not order, is due to the low coordination number (6). One could also argue that from the point of view of the $S = 2$ tetrahedron spin, the coordination number is only 4, and the smallest closed loop is a hexagon. Heisenberg spins on such a four–fold coordinated structure will probably not order.

We did not include the effects of long–range dipole–dipole interactions, which recently have been proposed to be responsible for the so–called dipolar spin–ice ground state. Our appraoch is valid in case $J_{nn} > D_D$ 2.5, so for systesm containing magnetic transition metal ions like spinel with magnetic ions on the B sublattice $ZnCr_2O_4$, $CsNiFeF_6$, $CsNiCrF_6$, $CsMnFeF_6$[29], $GeCu_2O_4$[67], LiV_2O_4 [68], than to systems with rare–earth iopns on a pyrochlore lattice.

We have found in various regions of parameter space re–entrant magnetic behaviour when lowering the temperature: non–magnetic (Paramagnetic) → Ferromagnetic → non–magnetic (Two-Dimer-Singlet or Tetrahedron Singlet). The high temperature phase is paramagnetic, while the low temperature phase is some type of spin fluctuating state. Such re–entrant behaviour has been reported as a function of the magnetic field for the garnet $Gd_3Ga_5O_{12}$ by [4, 5, 69, 70] and recently been discussed by Tsui et al[16].

The magnetization as a function of the field depends strongly on the model parameters. We find magnetization curves which show a single step for large field or a two step behaviour. Stepwise behaviour has been found for classical Heisenberg magnets by

Zhitomirsky et al [71]. See also the discussion of magnetization plateaus by Lhuillier and Misguich [32]. Such steps have been observed in various pyochlore systems[29, 30].

We have also calculated the specific heat for $s = 1/2$. Details of the calculation of the specific heat will be published elsewhere. For the zero-field specific heat of non–magnetic systems we find usually a single peaked Schottky–like anomaly, and in case of the re-entrant phase we find two peaks in the specific heat, possibly on top of a Schottky–like peak. Such peaks have recently been observed in the specific heat of $Gd_2Ti_2O_7$ [72].

Summarizing we find indications from this CVA of a rich magnetic behaviour for spins on the highly frustrated pyrochlore lattice as a function of tetragonal distortions: Two dimer singlet or tetrahedron ground states, re–entrant behaviour due to entropic ground state selection, magnetic field induced order Quantum Phase Transitions), together with steps in the magnetization as a function of field, Schottky like anomalies in the specific heat.

Acknowledgments

We acknowledge a grant from CNPq (300928/97–0). We also acknowledge Prof. Luciano Peixoto for critically reding the manuscript.

References

[1] P. Lacorre. *J. Phys. C: Solid State Phys.*, **20** :L775–L781, (1987).

[2] P.W. Anderson. *Mat. Res. Bull.*, **8**:153, (1973).

[3] P. Fazekas and P. W. Anderson. *Phil. Mag.*, **30**:23, (1974).

[4] A. P. Ramirez. *Strongly geometrically frustrated magnets. Annu. Rev. Mater. Sci.*, **24**:453, (1994).

[5] P. Schiffer and A. P. Ramirez. *Comments Cond. Mat. Phys.*, **18**:21, (1996).

[6] R. Moessner. *Can. J. Phys.*, **79**:1283–1294, (2001).

[7] C. H. Booth, J. S. Gardner, G. H. Kwei, R. H. Heffner, F. Bridges, and M. A. Subramanian. *Phys. Rev. B*, **62**:R755, (2000).

[8] H. Martinho, N. O. Moreno, J. A. Sanjurjo, C. Rettori, A. J. Garcia-Adeva, D. L. Huber, S. B. Oseroff, W. Ratcliff, S.-W. Cheong, P. G. Pagliuso, J. L. Sarrao, and G. B. Martins. *Phys. Rev. B*, **64** :24408, (2001).

[9] S. Franz, M. Mezard, Ricci-Tersenghi, M. Weigt, and R. Zecchina. *Europhys. Lett.*, **55** :465, (2001).

[10] A. P. Ramirez, C. L. Broholm, R. J. Cava, and G. R. Kowach. *Physica B*, **280**:290–295, (2000).

[11] Y. Yamashita and K. Ueda. *Phys. Rev. Lett.*, :to appear.

[12] O. Tchernyshyov, R. Moessner, and S. L. Sondhi. *Phys. Rev. Lett.*, **88** :67203, (2002).

[13] L. Bellier-Castella, M.J.P. Gingras, P.C.W. Holdsworth, and R.Moessner. *Can. J. Phys.*, **79**:1365–1371, (2001).

[14] M. J. Harris, S. T. Bramwell, P. C. W. Holdsworth, and J. D. M. Champion. *Phys. Rev. Lett*, **81**:4496–4499, (1998).

[15] K. Matsuhira, Z. Hiroi, T. Tayama, S. Takaga, and T. Sakakibara. *J. of Phys.: Cond. Mat.*, **14** :L559, (2002).

[16] Y. K. Tsui, J. Snyder, and P. Schiffer. *Phys. Rev. B*, **64** :12412, (2001).

[17] J. Villain, R. Bidaux, J. P. Carton, and R. J. Conteé. *J. Phys. (Paris)*, **41**:1263., (1980).

[18] J. Villain. *Z. Phys. B*, 33:21, (1979).

[19] R. R. Sobral and C. Lacroix. *Solid State Comm.*, **103**:407–409, (1997).

[20] J. N. Reimers, J. E. Greedan, and M. Björgvinsson. *Phys. Rev. B*, **45**:7295–7306, (1992).

[21] V. N. Kotov, M. E. Zhitomirsky, and O. P. Sushkov. *Phys. Rev. B*, **63**:64412, (2001).

[22] S. T. Bramwell and M. J. Harris. *J. Phys.: condens. matter*, **10**:1215–1220, (1998).

[23] R. Siddharthan, B. S. Shastry, A. P. Ramirez, A. Hayashi, R. J. Cava, and S. Rosenkranz. *Phys. Rev. Lett.*, **83**:1854, (1999).

[24] R. G. Melko, B. C. den Hertog, and M. J. P. Gingras. *Phys. Rev. Lett.*, **87**:67203, (2001).

[25] S. E. Palmer and J. T. Chalker. *Phys. Rev. B*, **62**:488, (2000).

[26] B. C. den Hertog and M. J. P. Gingras. *Phys. Rev. Lett.*, **84**:3430, (2000).

[27] M. J.P. Gingras and Byron C. den Hertog. *Can. J. Phys.*, **79**:1339–1359, (2001).

[28] V. Bondah-Jagalu and S. T. Bramwell. *Can. J. Phys.*, **79**:1381–1385, (2001).

[29] M. J. Harris and M. P Zinkin. *Mod. Phys. Lett.*, **10**:417–438, (1996).

[30] S. T. Bramwell, M. N. Field, M. J. Harris, and I. P. Paskin. *J. Phys. Condens. Matter*, **12**:483–495, (2000).

[31] S. T. Bramwell and M. J. P. Gingras. *Science*, **294**:1495, (2001).

[32] C. Lhuillier and G. Misguich. *Frustrated quantum magnets. lecture notes of the Cargese summer school on Trends in high magnetic field science (may (2001))*, .

[33] P. W. Anderson. *Phys. Rev.*, **102**:1008–1013, (1956).

[34] L. Pauling. *The Nature of the chemical bond*. Cornell University Press, Ithaca, 1938.

[35] R. J. Baxter. *Exactly Solved Models in Statistical Mechanics*. Academic Press, New–York, (1982).

[36] J. N. Reimers, A. J. Berlinski, and A.-C. Shi. *Phys. Rev. B*, **43**:865–878, (1991).

[37] J. N. Reimers. *Phys. Rev. B*, **45** :45, (1992).

[38] B. Canals and D. Garanin. *Can. J. Phys.*, **79**:1323–1331, (2001).

[39] R. Moessner and J. T Chalker. *Phys. Rev. B*, **58**:12049–12081, (1998).

[40] R. Moessner and J. T. Chalker. *Phys. Rev. Lett.*, **80**:2929, (1998).

[41] A.J. Garcia-Adeva and D.L. Huber. *Phys. Rev. Lett.*, **85**:4598, (2000).

[42] B. Canals and C. Lacroix. *Phys. Rev. B*, **61**:1149, (2000).

[43] B. Canals and C. Lacroix. *Phys. Rev. Lett.*, **80**:2933, (1998).

[44] H.Tsunetsugu. *J. Phys. Soc. Jpn.*, **70**:640–643, (2001).

[45] M. Elhajal, B. Canals, and C. Lacroix. *Can. J. Phys.*, **79**:1353–1357, (2001).

[46] M. Isoda and S. Mori. *J. Phys. Soc. Jp.*, **67**:4022, (1998).

[47] A. B. Harris, A. J. Berlinsky, and C. Bruder. *J. Appl. Phys.*, **96**:5200, (1991).

[48] E. Berg, E. Altman, and A. Auerbach. *Preprint*, .

[49] A.J. Garcia-Adeva and D. L. Huber. *Phys. Rev. B*, **63**:140404, (2001).

[50] A.J. Garcia-Adeva and D. L. Huber. *Phys. Rev. B*, **64**:14418, (2001).

[51] M. J. Harris, S. T. Bramwell, D. F. McMorrow, T. Zeiske, and K. W. Godfrey. *Phys. Rev. Lett.*, **79**:2554, (1997).

[52] J. M. Ziman. Cambridge University Press, Cambridge, 1979.

[53] E.N.M. Cirillo, G. Gonnella, M. Troccoli, and A. Maritan. *Journ. Stat. Phys.*, **94** :67–89, (1999).

[54] S. Yoshida, K. Nemoto, and K. Wada. *J. Phys. Soc. Jap.*, **71** :948–954, (2002).

[55] P. Chandra and B. Doucot. *J. Phys. A: Math. Gen.*, **27**:1541–1556, (1994).

[56] R. Melin, J. C. Angles d'Auriac, P. Chandra, and B. Doucot. *J. Phys. A: Math. Gen.*, **29** :5773–578, (1996).

[57] J. C. M. Henning. *Phys. Rev. B*, **21**:4983–4995, (1980).

[58] R. Moessner. *Phys. Rev. B*, **57**:R5587–R5589, (1998).

[59] L. Peixoto, private communication.

[60] D. C. Johnson, R. K. Kremer, M. troyer, X. Wang, A. Klumper, S. L. Dud'ko, A. F. Panchula, and P. C. Canfield. *Phys. Rev. B*, **61** :9558, (2000).

[61] A. B. Harris, C. Kallin, and A. J. Berlinsky. *Phys. Rev. B*, **45**:2899–2919, (1992).

[62] N. Bezakour, M. Hamedoun, M. Houssa, A. Hourmatallah, and F. Mahjoubi. *M. J. Condensed Matter*, **1**:2, (1999).

[63] G. S. Rushbrooke and P. J. Wood. *Mol. Phys.*, **1**:257, (1958).

[64] C. Pinettes, B. Canals, and C. Lacroix. *Phys. Rev. B*, **66** :24422, (2002).

[65] A. Koga and N. Kawakami. *Phys. Rev. B*, **63** :144432, (2001).

[66] N. Benzakour, M. Hamedoun, M. Houssa, A. Hourmatallah, and F. Mahjoubi. *phys. stat. sol. b*, **212** :335–342, (1999).

[67] T. Yamada, Z. Hiroi, M. Takano, M. Nohara, and Hidenori Takagi. *J. Phys. Soc. Jpn.*, **69**:1477–1483, (2000).

[68] V. Eyert, K.-H. Hoeck, S. Horn, A. Loidl, and P. S. Riseborough. *Europhys. Lett.*, **46**:762–767, (1999).

[69] O. A. Petrenko, C. Ritter, M. Yethiraj, and D. Paul. *Physica B*, **241-243** :727–729, (1997).

[70] O. A. Petrenko, D. M. Paul, C. Ritter, T. Zeiske, and M Yethiraj. *Physica B*, **266**:41, (1999).

[71] M.E. Zhitomirsky, A. Honecker, and O.A. Petrenko. *Phys. Rev. Lett.*, **85**:3269–3273, (2000).

[72] A. P Ramirez, B. S. Shastry, A. Hayashi, J. J. Krajewski, D. A. Huse, and R. J. Cava. *Phys. Rev. Lett.*, **89**:67202, (2002).

Table 1: The energy levels of the spins on a tetragonally distorted tetrahedron for $s = 1/2$.

S M L R	E(S,M,L,R)	S M L R	E(S,M,L,R)
0 0 0 0	0	2 $\pm$1 1 1	$6J - 3D + 4\Delta$
1 0 1 0	$2(J + D) + 2\Delta$	2 0 1 1	$6(J + D) + 4\Delta$
1 0 0 1	$2(J + D) + 2\Delta$	0 0 1 1	4Δ
1 $\pm$1 1 0	$2J - D + 2\Delta$	1 $\pm$1 1 1	$J - D + 4\Delta$
1 $\pm$1 0 1	$2J - D + 2\Delta$	1 0 1 1	$2(J + D) + 4\Delta$
2 $\pm$2 1 1	$6J - 6D + 4\Delta$		

Table 2: Energies in units of J obtained from approximate calculations on a quintet cluster of tetrahedra for AF exchange interactions. For details see the text. The degeneracy and spin of each state are indicated in parenthesis. In the row NS we indicate the number of total spin states and the number of local spin states present in each calculation. The total number of states with $M_Q = 0$ is 12870. The energies should be corrected by -12. The exact ground state energy has been calculated by [59].

(S, D, Q, M_Q)	(0,0,0,0)	(1,1,1,0)	(1,1,1,0)	(1,1,1,0)	(1,1,1,0)	exact
S_{sum}	0	1	2	3	4	
$NS =$	16/1296	112/9232	520/9232	1192/9232	1597/9232	12870
1	-0.188(16;0)	-0.235(16;0)	-0.830(16;0)	-0.830(16;0)	-0.856(16;0)	-0.82(16;0)
2	–	1.500(48;1)	0.939(48;1)	0.767(32;1)	0.712(28,1)	0.69(48;1)
3	–	1.812(32;1)	1.690(32;1)	0.938(16;1)	0.750(1,1)	1.23(32;1))
4	–	2.797 (16;1)	2.000(32;0)	1.448(32;1)	0.755(1,1)	1.77(32;0)
E_{ST}	–	1.733	1.768	1.597	1.568	1.51

Table 3: The ground state energy per site and singlet triplet gap ΔE_{ST}, both in units of J.

E_G	ΔE_{ST}	method	ref.
-0.96	–	J'/J Expansion	[65]
-0.916	1.688	J'/J Expansion	[46]
-1.00	–	J'/J Expansion	[45]
-1.144	–	Spin-Waves	[19]
-0.975	–	Mean Field	[47]
-1.0?	1.10	J'/J Expansion	[44]
-1.12	–	J'/J Expansion	[42]
-1.10	1.4	Exact 16 site	[43]
-1.12?	0.8	SuperTetrahedron: 16 sites	[48]

Table 4: The b coefficients for $s = 1/2$ for the tetrahedron as basis cluster.

S	0	1	1	1	1	1	1	0	1	1	1	2	2	2	2	2
M	0	-1	0	1	-1	0	1	0	-1	0	1	-2	-1	0	1	2
L	0	0	0	0	1	1	1	1	1	1	1	1	1	1	1	1
R	0	1	1	1	0	0	0	1	1	1	1	1	1	1	1	1
$m = -1/2$	1	0	0	0	1/2	0	-1/2	0	1/4	0	-1/4	1/2	1/4	0	-1/4	-1/2
$m = 1/2$	1	0	0	0	-1/2	0	1/2	0	-1/4	0	1/4	-1/2	-1/4	0	1/4	1/2

Table 5: Critical coordination number Z_{crit} and critical temperature in the pair–CVA $T_{c,pair}/T_{c,MF}$ the tetrahedron–CVA $T_{c,H}/T_{c,MF}$ for ferromagnetic nn Heisenberg exchange J and the ratio of the Ising and Heisenberg critical temperature $T_{c,I}/T_{c,H}$ on the pyrochlore lattice – the Curie–Weiss mean field value is: $k_BT_c = 2JZs(s+1)/3$ for $Z = 6$. The critical temperature in the Heisenberg limit (zero–field zero) ($k_BT_{c,H}/J$) and in the Ising limit ($k_BT_{c,I}/J$) for $D_s/J = 5000$. The ratio $T_{c,I}/T_{c,H}$ is in the mean field approximation this ratio is $(1 + 1/S)/3$. The high temperature expansion is derived from the formula of Rushbrooke and Wood [63]. In the last two rows we give the characteristic critical values for the tetrahedral zero–field D_T.

$s =$	1/2	1	3/2	2	5/2	3	7/2
Pair–CVA with pairs, ferromagnetic Heisenberg spins:							
Z_{crit}	4	3	2.66	2.4	2.3	2.26	2.25
$T_{c,pair}/T_{c,MF}$	0.607	0.737	0.773	0.788	0.796	0.801	0.804
Tetrahedron–CVA with ferromagnetic Heisenberg (H) and Ising (I) spins:							
$k_BT_{c,H}/J$	0	-4.664	-9.636	-16.001	-23.980	-32.955	-43.566
$k_BT_{c,I}/J$	0	-8.808	-19.818	-35.234	-55.054	-79.277	-107.906
$T_{c,H}/T_{c,MF}$	0	0.583	0.642	0.667	0.679	0.687	0.692
$T_{c,I}/T_{c,H}$	NA	1.888	2.056	2.208	2.295	2.406	2.477
High temperature expansion Heisenberg model $Z = 6$ ferromagnetic:							
k_BT_c/J	0.629	0.684	0.699	0.705	0.709	0.711	0.712

Table 6: In this table we give the characteristic critical values for the tetrahedral zero–field $D_{T,max}$ and the maximum critical temperature T_{max} which characterizes the re–entrant regiion for $s = 1/2$ to $7/2$. See figure 10.

T_{max}/J(max)	NA	-2.647	-5.128	-8.143	-12.400	-15.662	-20.137
$D_{T,max}/J \times 100$(max)	NA	-3.695	-6.312	-7.985	-9.378	-9.982	-10.465

Figure 1: The pyrochlo (=B sublattice of the spinel structure) lattice. We have indicated the Corner–Sharing–Tetrahedra in blue, and some of the hexagon loops. The cubes (black thin lines) are drawn to guide the eye

Figure 2: The tetrahedron with site and bond indices as used in the main text. The local trigonal $\langle 111 \rangle$ quantization axes and a tetragonal axis (C_2 or S_4) are also indicated.

Figure 3: In this figure we illustrate the energy levels of spin states on a tetrahedron for $s = 1/2$. The exchange interaction is $J = 1$, the reduced tetragonal anisotropy is $d_T = D_T/J$, and the reduced exchange anisotropy is $\delta = \Delta/J$. The reduced magnetic field is $h = \mu_B H/J$. The magnetic field is along a tetragonal axis. The (L, R) character of the states is indicated in parenthesis, the degeneracy is indicated in brackets. For the energies see also table: 1.

Figure 4: The ground state phase diagram for ferromagnetic (F) and anti ferromagnetic (AF) *nn* exchange interactions for $s = 1/2$, in the d_T–δ plane. The numbers in parenthesis indicate the L, R character of the ground state. The equations separating the various ground states are given in the main text.

Figure 5: The reduced critical temperature $k_B T_c/J$ as a function of $C_t = 2(Z_t - 1)/Z_t$ for ferromagnetic nn exchange for $s = 1/2$; Z_t is the coordination number. The case of 2, 3 and 4 CST is $C_t = 1$, 4/3 and 1.5, respectively, are indicated as squares.

Figure 6: Detail of the ferromagnetic phase diagram for $s = 1/2$ in the d_T–δ plane. We have indicate in black the region with re–entrant behaviour, which separates the singlet (S) ground state region from the ferromagnetic (F) ground state region.

Figure 7: The reduced critical temperature $k_B T_c/J$ as a function of the reduced tetrahedral anisotropy $d_T = D_T/J$ for various values of the reduced exchange anisotropy $\delta = \Delta/J = 0., -1, -1.5, -2.0, -2.5, -3.0$ for $s = 1/2$. Paramagnetic (P), Ferromagnetic (F) and singlet–like or collective paramagnetic (S) behaviour of the spin system is indicated. See also figure 6 and table 5. In this graph we have also indicated the curves, for the same set of δ values, below which the entropy becomes negative: T_S.

Figure 8: The number of states accessible as a function of the temperature for ferromagnetic exchange (F) and anti–ferromagnetic exchange (AF).

Figure 9: The temperature T_S for which the entropy vanishes for non–magnetic spin system for ferromagnetic exchange $J = -1$ as a function of the tetragonal anisotropy d_T, for magnetic fields $h = 0$, 1 and 2, along the line A-C in the phase diagram 4.

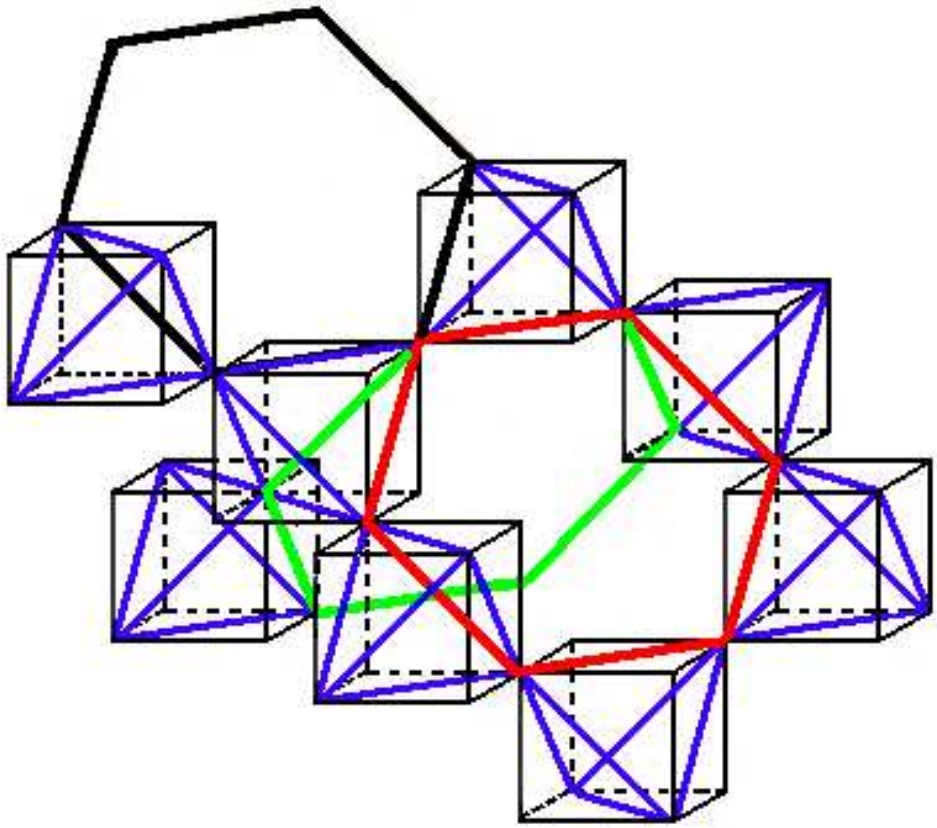
Figure 10: The reduced critical temperature $k_B T_c/J$ as a function of the reduced tetragonal anisotropy $d_T = D_T/J$ for $s = 3/2$ and reduced tetrahedral anisotropy. Paramagnetic (P), Ferromagnetic (F) and singlet–like or collective paramagnetic (S) behaviour of the spin system is indicated. The maximum temperature and anisotropy values given in table 5.
are indicated.

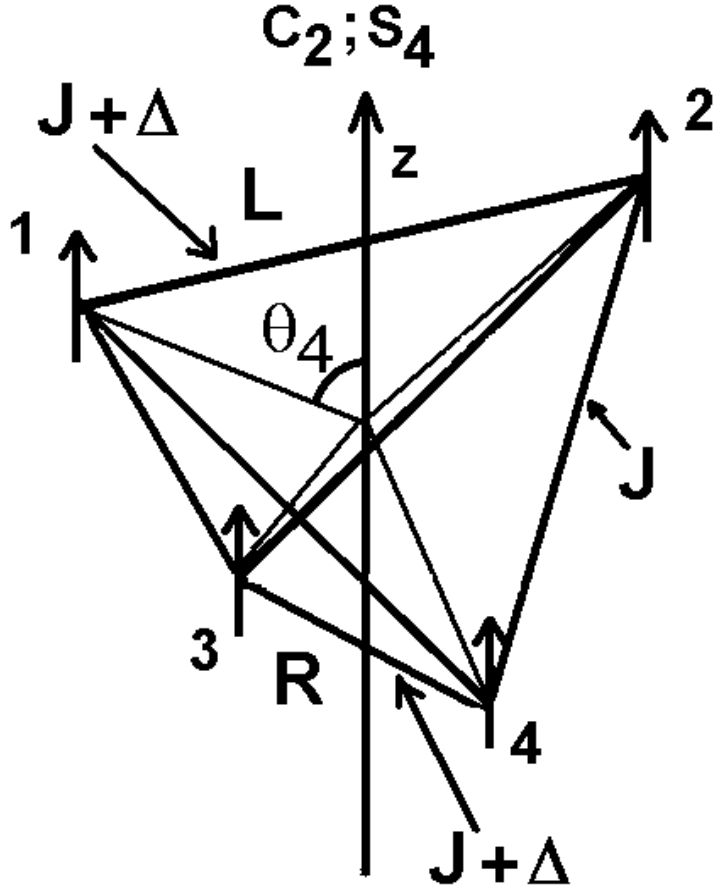
Figure 11: The magnetization $\mathcal{M}$ as a function of the magnetic field h for ferromagnetic exchange $J = -1$ using equation 2.46, for three temperatures $T = 0.1$, 1 and 5, for various values of the tetrahedral anisotropy $|d_T| = 0.05, 0.1, 0.25, 0.5, 1.0, 2.0$ for $\delta = -3$ (line A-C in fig. 4) and $\delta = 1$ (line B-D in fig. 4). A: $\delta = -3$, d_T positive; B: $\delta = 1$, d_T: negative; C: $\delta = -3$, d_T: negative; D:$\delta = 1$, d_T: positive. For details see the text.

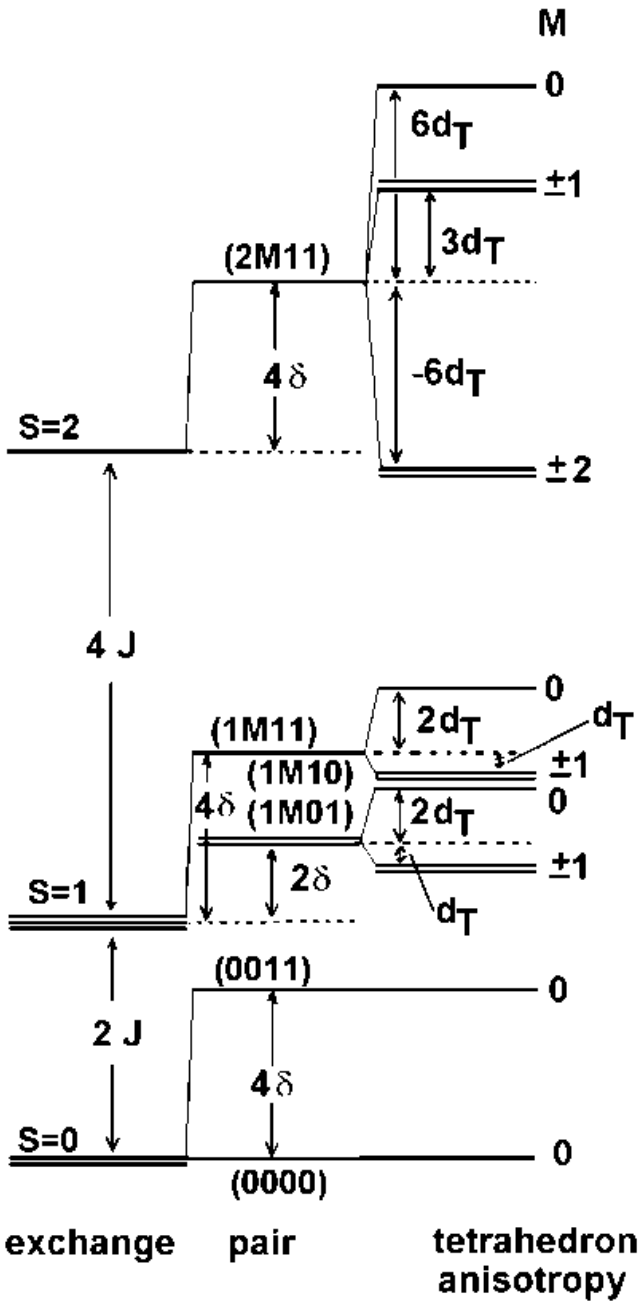
Figure 12: The magnetization $\mathcal{M}$ in the re–entrant region for ferromagnetic nn exchange $J = -1$ for $s = 1/2$ in small field $h = 0.001$ for $\delta = -3$ for various values of the tetragonal anisotropy from $d_T = -0.85$ to -1.075 with steps of -0.025. Units used: $|J|$.

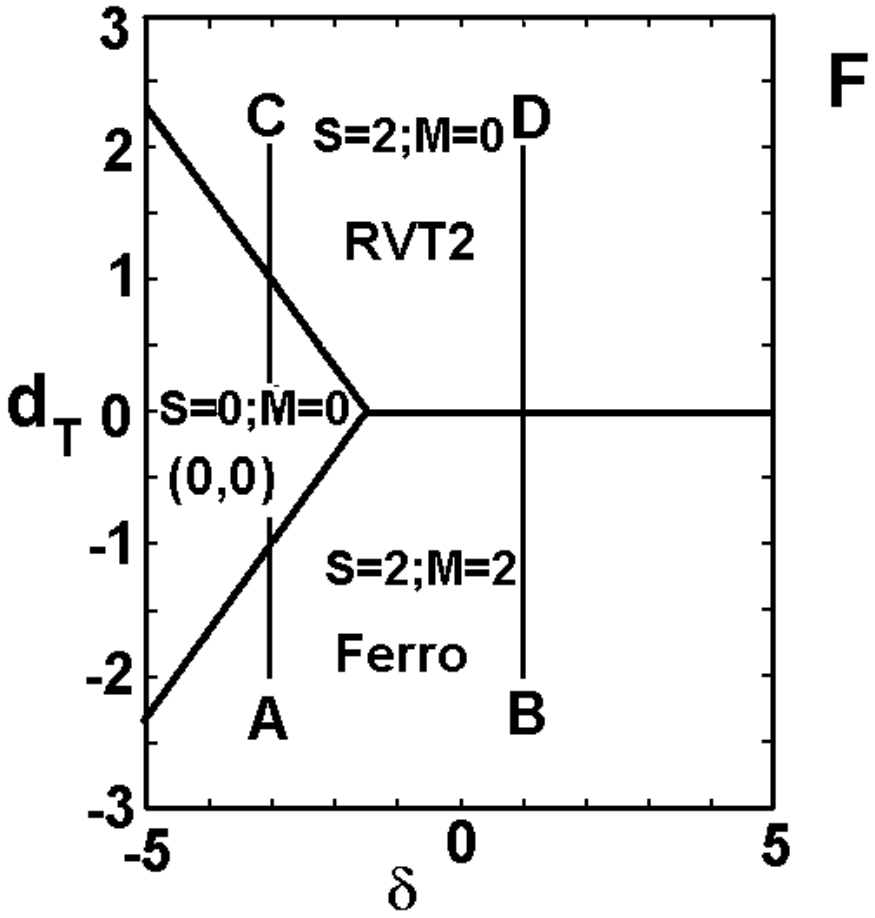
Figure 13: The magnetization $\mathcal{M}$ as a function of temperature for ferromagnetic exchange $J = -1$ using equation 2.46, for the magnetic fields $h = H/|J| = 0.01, 1, 2, 3, 5, 10$, for various values of the tetrahedral anisotropy $d_T = 0.05, 0.1, 0.25, 0.5, 1.0, 2.0$ for $\delta = 1$ (line B-D in fig. 4). For details see the text. Units used: $|J|$.

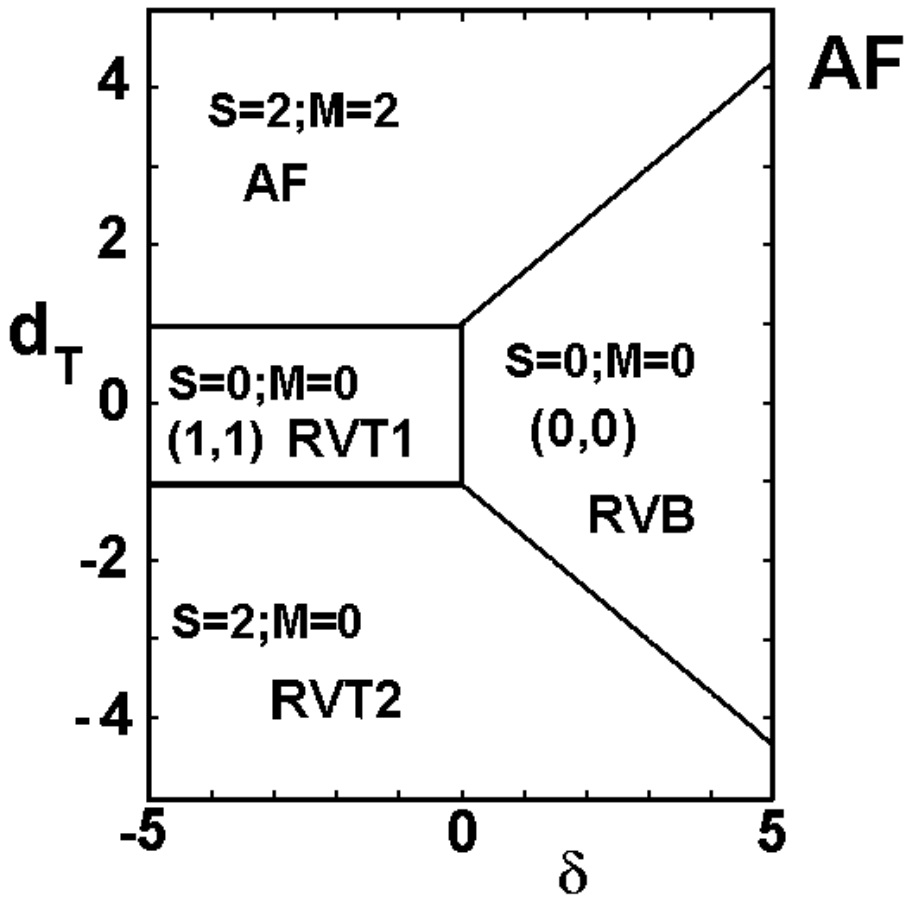
Figure 14: The specific heat as a function of temperature for small magnetic field in the re–entrant regiion for $\delta = -3$ and $d_T = 0.925$.

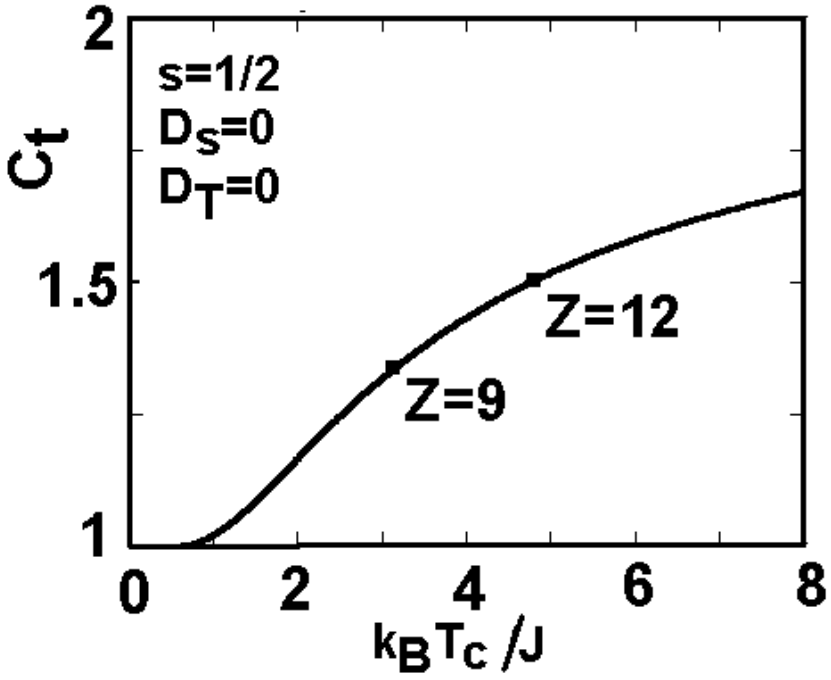


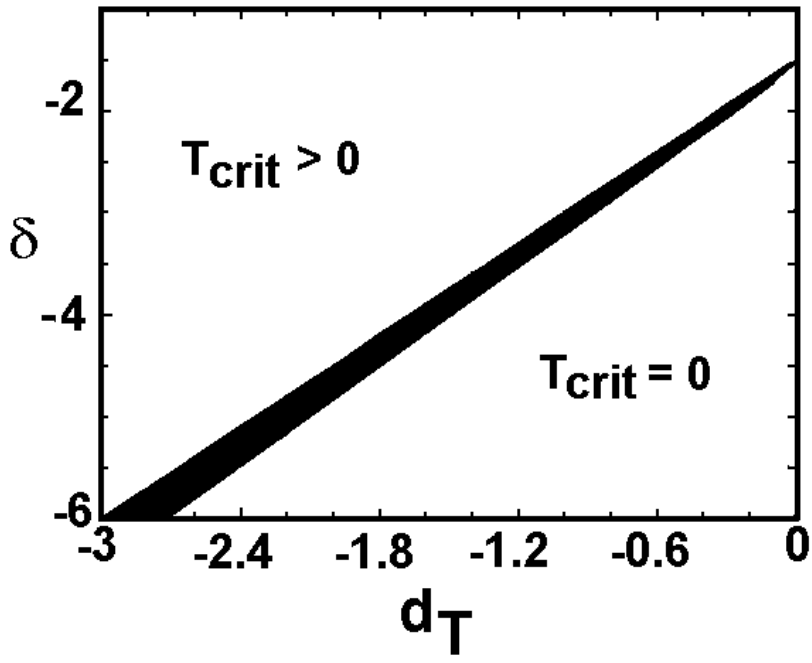

C2;S4
J+Δ
z
2
L
1
θ4
J
3
R
4
J+Δ

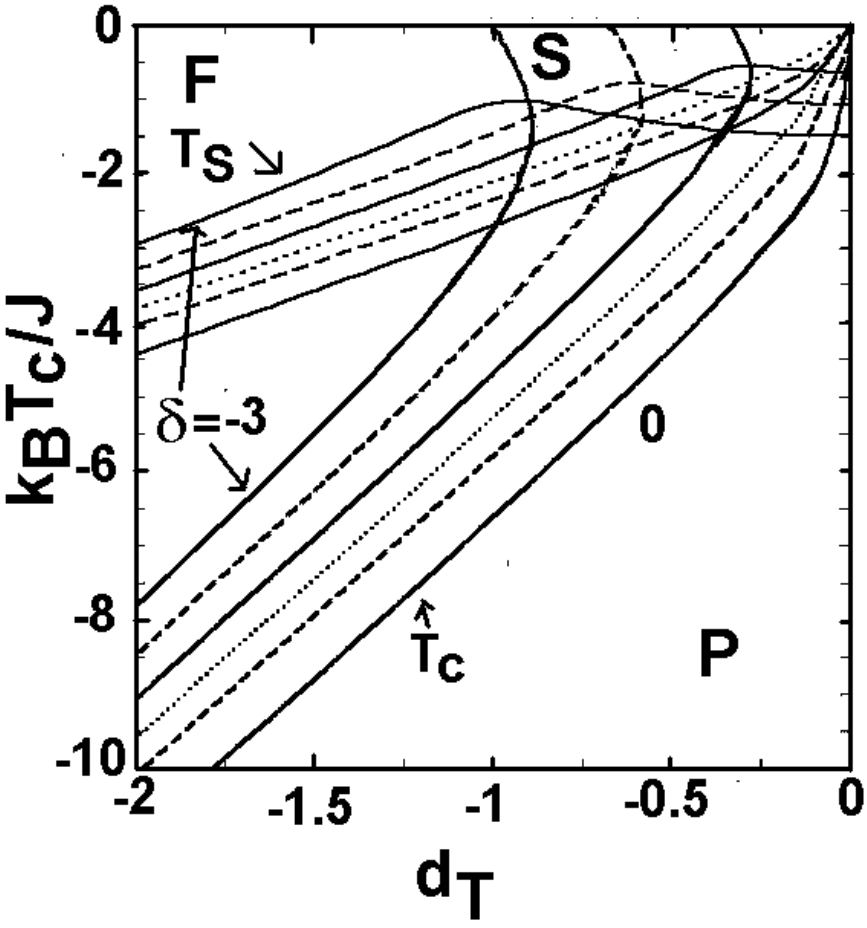

M
0
6d_T
±1
3d_T
(2M11)
4δ
-6d_T
S=2
±2
4 J
0
2d_T
d_T
(1M11)
(1M10)
±1
4δ
(1M01)
0
2d_T
2δ
±1
S=1
d_T
(0011)
0
2 J
4δ
S=0
0
(0000)
exchange
pair
tetrahedron
anisotropy

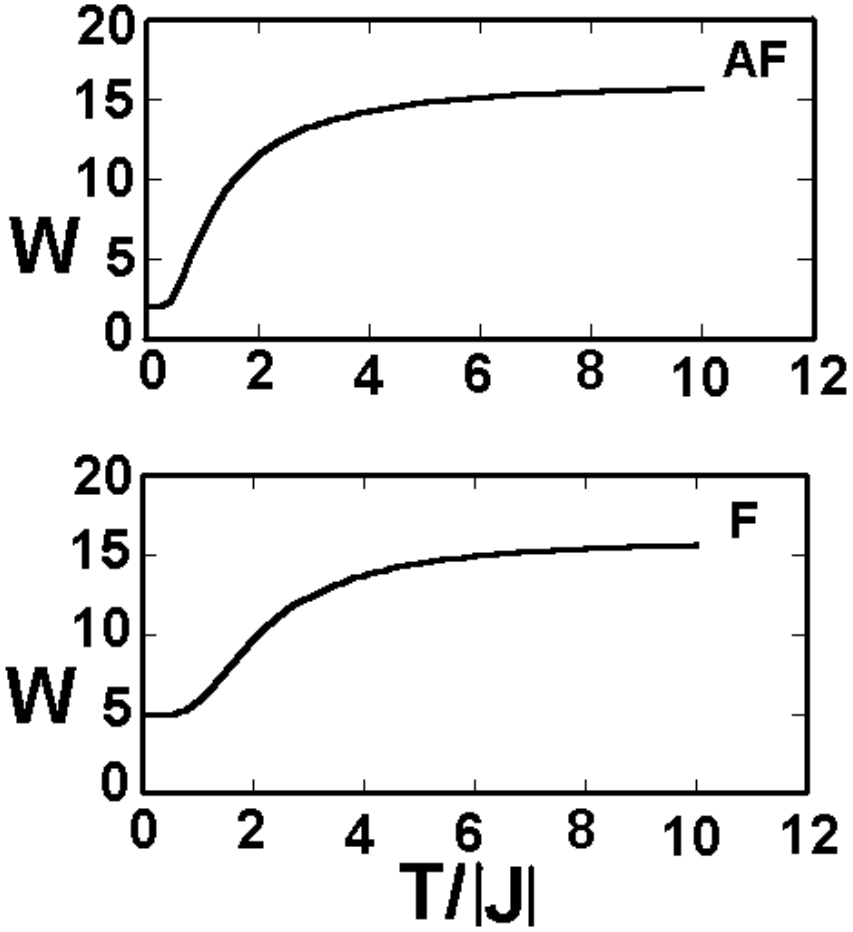

F
C
D
S=2;M=0
RVT2
S=0;M=0
(0,0)
S=2;M=2
Ferro
A
B
d_T
δ
3
2
1
0
-1
-2
-3
-5
0
5

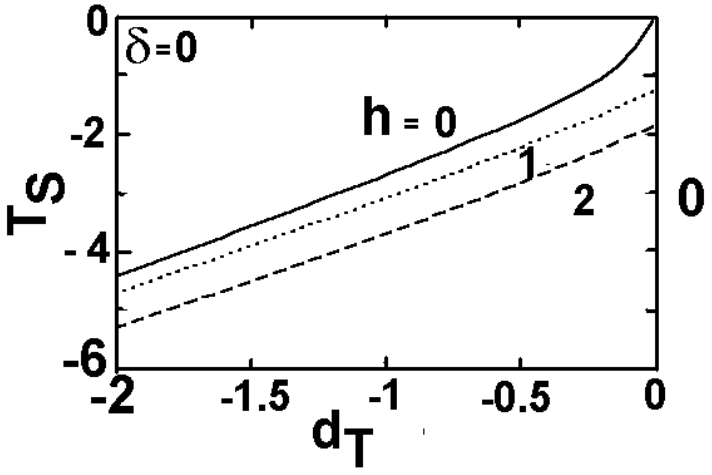

AF
S=2;M=2
AF
S=0;M=0
(1,1) RVT1
S=0;M=0
(0,0)
RVB
S=2;M=0
RVT2
d_T
δ
4
2
0
-2
-4
-5
0
5

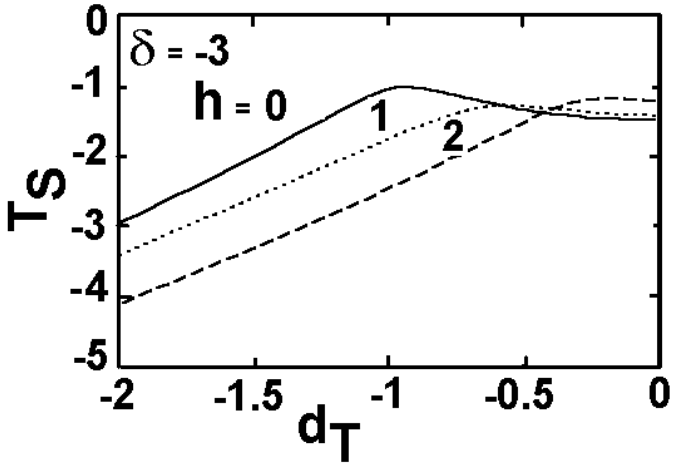

2
1.5
1
C_t
s=1/2
D_S=0
D_T=0
Z=12
Z=9
0
2
4
6
8
$k_B T_C$ /J

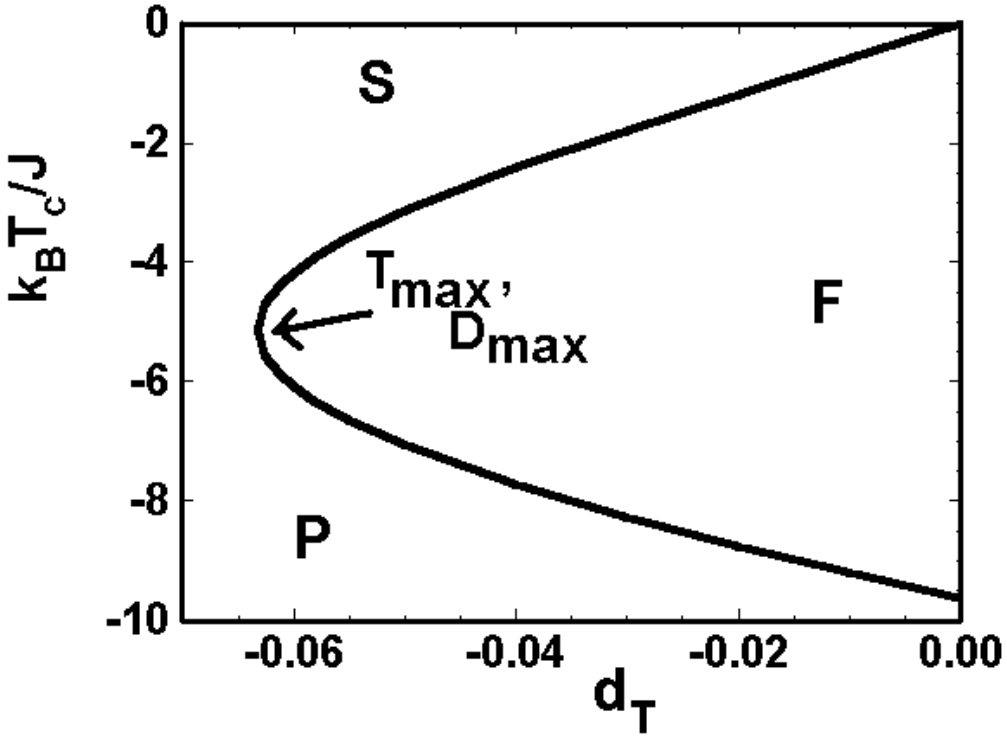

-2
-4
-6
δ
$T_{crit} > 0$
$T_{crit} = 0$
-3
-2.4
-1.8
-1.2
-0.6
0
d_T

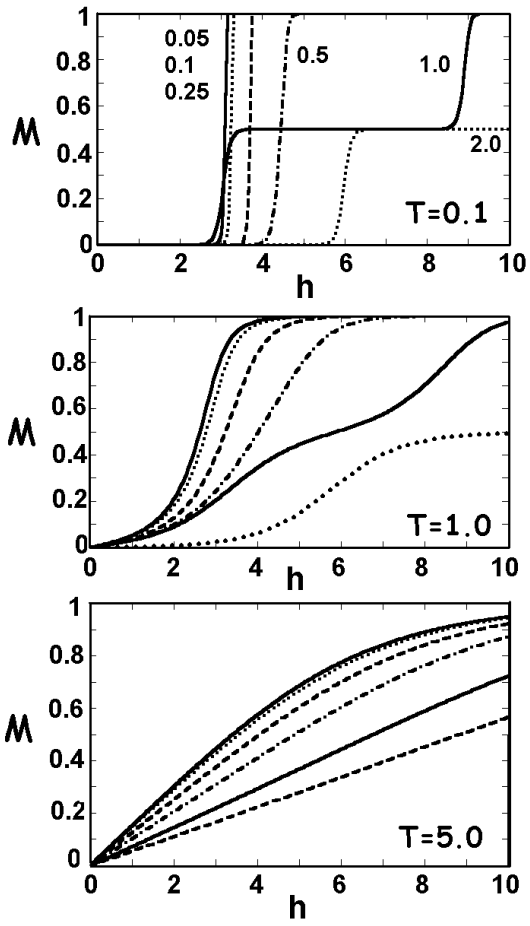

F
S
T_S
δ=-3
0
P
T_c
k_BT_c/J
d_T
0
-2
-4
-6
-8
-10
-2
-1.5
-1
-0.5
0

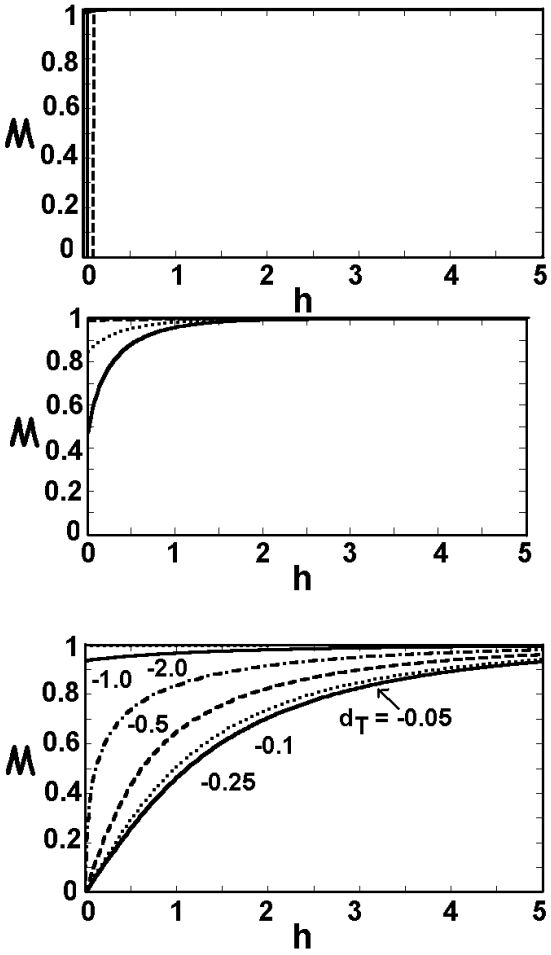

20
15
10
5
0
W
AF
0
2
4
6
8
10
12
20
15
10
5
0
W
F
0
2
4
6
8
10
12
T/|J|

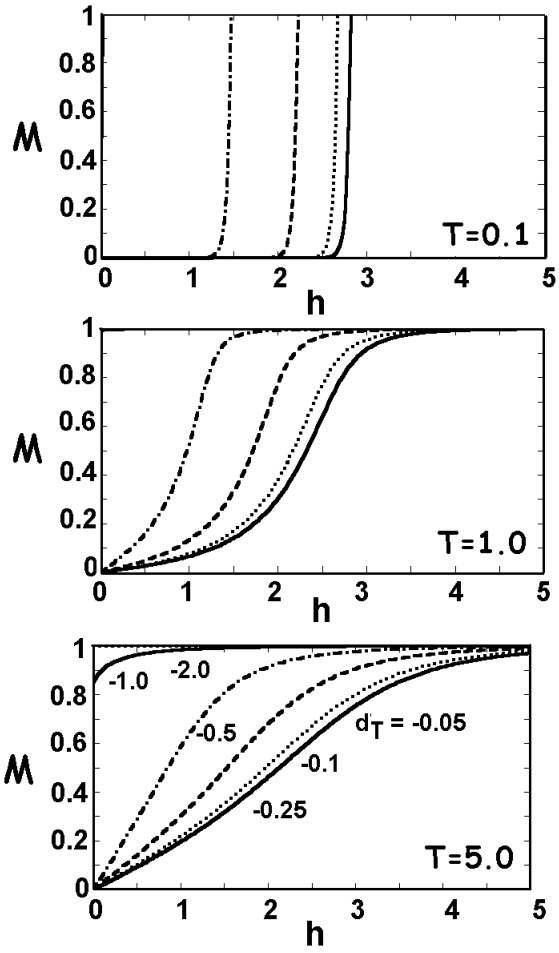

δ=0
h = 0
1
2
0
Ts
0
-2
- 4
-6
-2
-1.5
-1
-0.5
0
dT

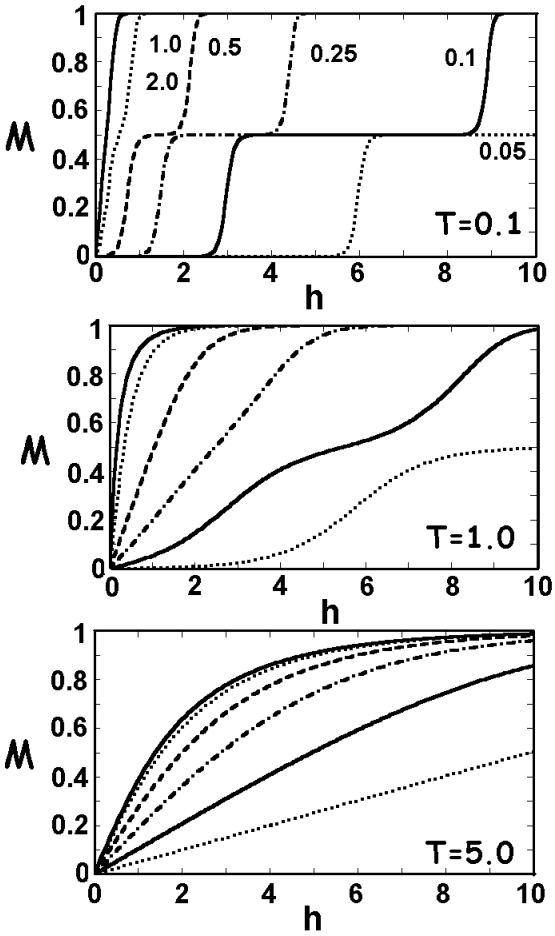

δ = -3
h = 0
1
2
Ts
0
-1
-2
-3
-4
-5
-2
-1.5
-1
-0.5
0
dT

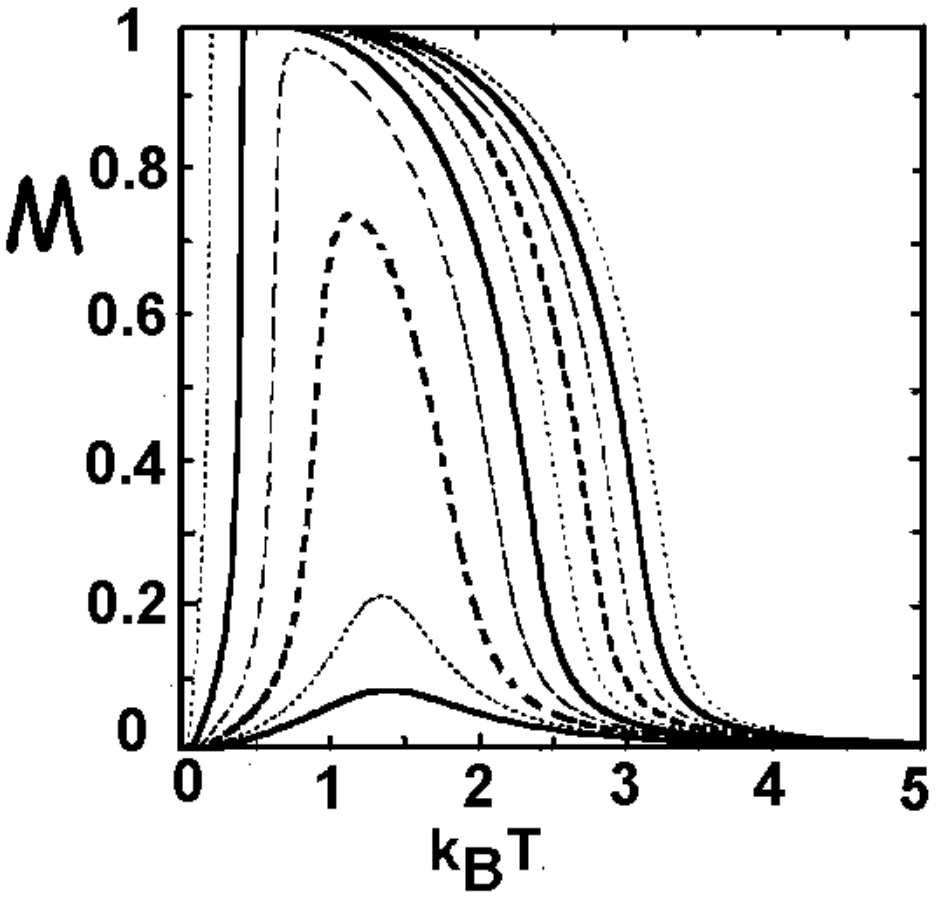

0
-2
-4
-6
-8
-10
S
F
P
T_{max} ,
D_{max}
$k_B T_c/J$
-0.06
-0.04
-0.02
0.00
d_T

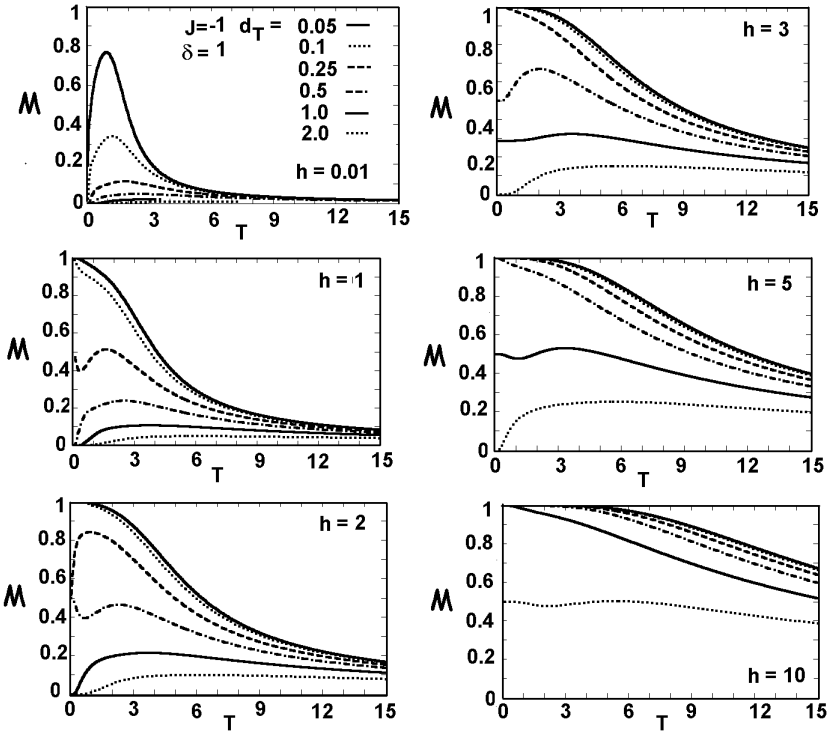

M
h
0.05
0.1
0.25
0.5
1.0
2.0
T=0.1
T=1.0
T=5.0

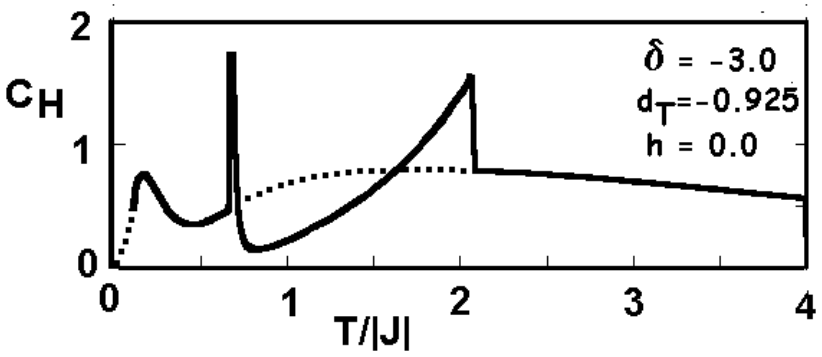

M
h
0
0.2
0.4
0.6
0.8
1
0
1
2
3
4
5
-1.0
-2.0
-0.5
-0.1
-0.25
d_T = -0.05

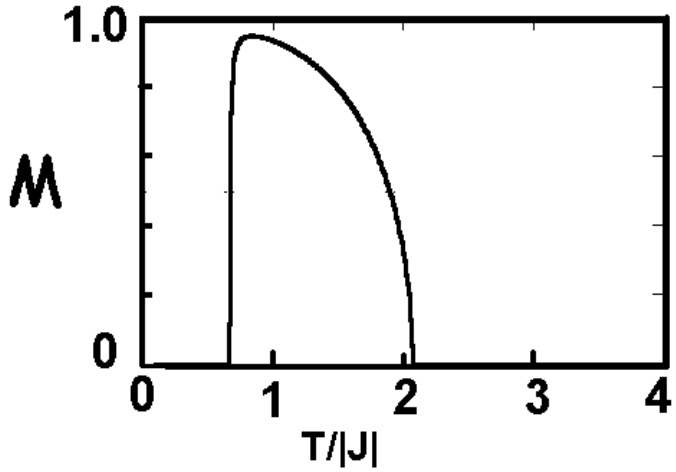

M
h
T=0.1
T=1.0
T=5.0
-1.0
-2.0
-0.5
-0.1
-0.25
d_T = -0.05


M
h
T=0.1
1.0
2.0
0.5
0.25
0.1
0.05
T=1.0
T=5.0


M
1
0.8
0.6
0.4
0.2
0
0
1
2
3
4
5
$k_B T$


J=-1
δ = 1
d_T = 0.05
0.1
0.25
0.5
1.0
2.0
h = 0.01
h = 3
h = 1
h = 5
h = 2
h = 10
M
T


2
1
0
C_H
δ = -3.0
d_T=-0.925
h = 0.0
0
1
2
3
4
T/|J|


1.0
M
0
0
1
2
3
4
T/|J|